Geochemical Journal, Vol. 47, pp. 547 to 565, 2013 doi:10.2343/geochemj.2.0277

Growth rate of continental crust in the northeast margin of the North China Craton: Constraints from the U–Pb dating and Lu–Hf isotopes of detrital zircons from the Laoha River

CHUANG BAO, YUELONG CHEN,* RUI GUO and DAPENG LI

School of Earth Sciences and Resources, China University of Geosciences, Beijing 100083, PR China

(*Received April 19, 2013; Accepted July 26, 2013*)

Recently, how to quantitatively estimate the growth rate of continental crust is an enigmatic issue. With the development of ICP-MS technology, the U–Pb dating and Lu–Hf isotopic compositions of detrital zircons from the fluvial sediments can provide an effective and simple approach to constrain the growth rate and evolutionary history of continental crust. In this paper, 189 concordant detrital zircons from the Laoha River have been analyzed for U–Pb ages and Lu–Hf isotopic compositions by excimer LA-MC-ICP-MS. Detrital zircons from samples LH and LH2 show three major age groups, i.e., 2370 Ma~2572 Ma, 1728~2087 Ma, 127~376 Ma and 2374~2598 Ma, 1765~2087 Ma, 119~405 Ma, respectively. They have the common prominent two stage Hf model ages with a peak at *ca*. 2.7 Ga, which is consistent with the global continental crust. These indicate that the timing of the strongest magmatic events is at *ca*. 2.5 Ga and 1.8 Ga, and the best estimation age of mantle extraction of the northeast margin of North China Craton is *ca*. 2.7 Ga. The detrital zircons with U–Pb ages of ~1.8 Ga and ~2.5 Ga have the two stage Hf model ages of *ca*. 2.7 Ga, whereas $\varepsilon_{Hf}(t)$ values are different from those of depleted mantle. These indicate that the majority of continental crust of the northeast margin of North China Craton at time of ~1.8 Ga originated from the reworking of ~2.7 Ga crust. About 5% of the present crustal volume in the northeast margin of North China Craton was formed at 2.9 Ga; whilst ~64% of the present crustal volume in the northeast margin of North China Craton has been formed at 2.5 Ga, which is higher than that of previous studies. It suggests that the continental crust growth in the North China Craton is not uniform, but it is consistent with the episodic growth of global continental crust (60%). Moreover, the majority continental crust of the northeast margin of North China Craton has been formed at 1.8 Ga (84%) as previously interpreted. Finally, we have used formulas to quantitatively calculate the reworking rate and give a suggestion that the time of 2.5 Ga is also the main growth period of continental crust of the North China Craton, and the time of 1.8 Ga is the strongest reworking period of the continental crust in the craton. In addition, the reworking rate began to drop after reactivating in the North China Craton, and the addition of depleted mantle was gradually increased.

Keywords: North China Craton, detrital zircon, U–Pb age, Hf isotope, Laoha River

INTRODUCTION

The growth rate of continental crust remains controversial, with two opposite hypothetical models of which the most widely accepted one is that the majority of continental crust began to form after 4.0 Ga and has been growing irreversibly since then (Moorbath, 1977; Fyfe, 1978; McLennan and Taylor, 1982; Hawkesworth and Kemp, 2006; Kemp *et al*., 2006; Wang *et al*., 2009; Yang *et al*., 2009; Dhuime *et al*., 2012). According to previous studies, the continental crust in the early Precambrian has several main growth periods, 3.6 Ga, 2.7 Ga, 1.8 Ga and 1.2 Ga (McCulloch and Bennett, 1994; Condie, 1998, 2000). The fastest continental crust growth period of the North China Craton is ~2.7 Ga (Wu *et al*., 2005; Yang *et al*., 2009; Geng *et al*., 2012; Peng *et al*., 2012, 2013; Wang *et al*., 2012, 2013; Zhao and Zhai, 2013; Zheng *et al*., 2013; Bao *et al*., 2013). The other hypothesis is that the mass of continental crust that formed between 4.0 Ga and 4.5 Ga was similar to today's and has been a steady-state since then with continental crust being recycling into the mantle as fast as it forms (Armstrong and Harmon, 1981; Armstrong, 1991; Wang *et al*., 2009; Yang *et al*., 2009).

In recent years, how to quantitatively estimate the growth rate of continental crust is an enigmatic issue (Iizuka *et al*., 2010; Dhuime *et al*., 2012). With the development of ICP-MS technology, the U–Pb dating and Lu–Hf isotopic compositions of detrital zircons from flu-

*Corresponding author (e-mail: chyl@cugb.edu.cn)

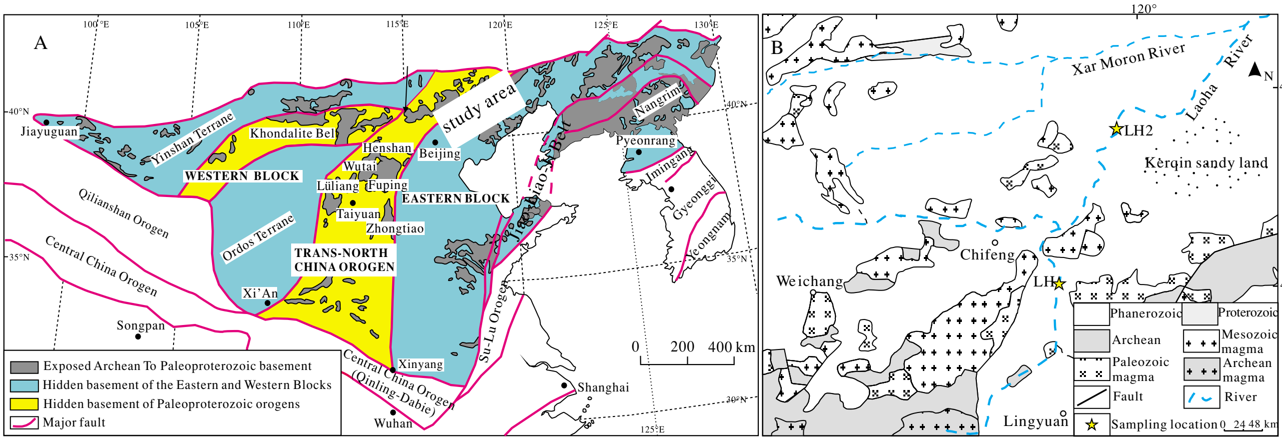

Fig. 1. Simplified map of the North China Craton (A) (Zhao et al., 1998, 1999) and Laoha River basin (B).

vial sediments can provide a new perspective on the growth rate of continental crust. Because the fluvial sediment composition can reveal information about provenances of sediments, and zircons from fluvial sediments can be resistant to chemical weathering and mechanical abrasion, so they can survive weathering from their protoliths to river mouths where a single sample can provide information about the sources of an entire river basin (Rino *et al*., 2004; Wang *et al*., 2009; Yang *et al*., 2009). In the last decades, although extensive investigations have been carried out on the formation and evolution of the North China Craton, which led to discovery three Paleoproterozoic continent-continent collisional belts (Khondalite Belt, Trans-North China Orogen and Jiao-Liao-Ji Belt) (Wan *et al*., 2000, 2006a, 2012b; Zhao *et al*., 2000, 2011; Guan *et al*., 2002; Guo *et al*., 2005, 2012; Xia *et al*., 2006; Zhang, J. *et al*., 2006, 2007, 2009, 2012; Jian *et al*., 2012; Zhao and Guo, 2012), most of these investigations were focused on tectonic processes operative during the amalgamation of microcontinental blocks along these collisional belts, but few studies were concentrated on the accretion of the North China Craton, and especially on the accretion rates.

Yang *et al*. (2006) applied fluvial sediments to constrain the evolution of continental crust in China. 110 concordant zircons from the Hanjiang River of Shanxi Province were used to constrain the evolution of northern Yangtze Craton, south China. Unfortunately, the Lu–Hf isotopes of detrital zircons were not determined in the study.

Yang *et al*. (2009) collected the fluvial sediments from the Yongding River, Luan River and Yellow River to constrain the episodic growths of the North China Craton, but the Yellow River and Luan River do not drain entirely within the North China Craton, and thus they could not entirely reveal the information of North China Craton. Meanwhile, the Yongding River drains mainly in the central North China Craton, so it also could not be used to reveal the growth rate of northeast margin of North China Craton.

Diwu *et al*. (2012) measured 187 detrital zircons in two samples from the lower reach of the Jing River and the Luo River to characterize the crustal growth history of the West Block of North China Craton. In his paper, about 60% of the present crustal volume of the North China Craton was generated in the between Mesoarchean and Late Neoarchean (3.0 to 2.5 Ga), and their results revealed that ~2.7 Ga and ~2.5 Ga are the most prominent time of magmatism and the period of continental rapidly growth, respectively. Meanwhile, the continental crust of the North China Craton that formed at 2.5 Ga, is not a reworking component, and it is a juvenile crust.

In this paper, we collected two fluvial sedimentary samples from the Laoha River that it drains entirely within the northeast margin of North China Craton to determine U–Pb ages and Lu–Hf isotopic compositions of detrital zircons, and the fluvial sediment can provide an effective sample of an entire river basin and can reveal information about its source areas. So the data can be used to calculate the continental crust growth rate and identify periods of crustal growth of the preserved continental crust in the Laoha River basin.

Geological Setting and Sampling

The Laoha River, which is 873 km long, originates from Pingquan County of Hebei Province, and interflows with Xar Moron River in the Inner Mongolia, China (Fig. 1). In the northeast of the Laoha River, Kerqin Sandy Land has the detrital zircons that derived from Xing–Meng Orogenic Belt (Xie *et al*., 2007). According to the geotectonic location, the Laoha River drains entirely in the northeast margin of North China Craton, so it can reveal the geological information of the northeast margin of North China Craton.

The North China Craton is one of the oldest rocks in the word. Major progress in understanding the geological history and tectonic division of North China Craton has been made in the past few years (Zhao *et al*., 2011; Guo *et al*., 2012; Jian *et al*., 2012; Wan *et al*., 2012b; Zhao and Guo, 2012). The oldest age of rock in the North China Craton is 3.8 Ga, which have been found in the Anshan area of Liaoning Province (Liu *et al*., 1992; Song *et al*., 1996; Wan *et al*., 2005), and the oldest zircon age in the North China Craton is *ca*. 3.85 Ga, which was also found in the Anshan area of Liaoning Province (Liu *et al*., 1992; Yang *et al*., 2009). According to the Nd and Hf isotopes, the best estimation age of mantle extraction of the North China Craton is 2.7 Ga (Wu *et al*., 2005; Yang *et al*., 2009; Geng *et al*., 2012; Diwu *et al*., 2012; Sun *et al*., 2012; Ma *et al*., 2013; Wang *et al*., 2013), but the U–Pb ages in the North China Craton indicated that the strongest magmatic events occurred at ~2.5 Ga and the much of continental crust in the North China Craton has formed at that time (Liu *et al*., 1990; Zhao *et al*., 2002; Kröner *et al*., 2005; Yang *et al*., 2009; Wan *et al*., 2010, 2012a; Geng *et al*., 2012; Diwu *et al*., 2012). The West Block of the North China Craton has formed with the collision between Yinshan and Erdos Blocks at 1.95~1.90 Ga (Zhao *et al*., 2005; Wan *et al*., 2006a, 2010; Yang *et al*., 2009), and the united Western Block collided with the Eastern Block at ~1.85 Ga, (Wan *et al*., 2000, 2006a; Zhao *et al*., 2000; Guan *et al*., 2002; Guo *et al*., 2005; Xia *et al*., 2006; Zhang, J. *et al*., 2006, 2007, 2009, 2012). After that, the North China Craton completed cratonization, indicating that the carton could remain quiescent with zero to negligible growth. However, recent studies have revealed that the North China Craton has been reactivated during Phanerozoic times (Gao *et al*., 2002; Wu *et al*., 2003; Zheng *et al*., 2005; Zhang, S. H. *et al*., 2007).

In the upper reach, fluvial sediments can reveal the information about the near sources of river. In the lower reach, fluvial sediments can reveal the information about the whole river basin, because it has a big catchment area. In order to avoid the difference resulting from the upper and lower reaches, we collected two floodplain samples in this river. The upper and lower reaches are located in 119°22.458′ E, 42°04.386′ N and 119°42.431′ E, 42°45.548′ N, respectively (Fig. 1).

Analytical Methods

Zircons from >5 kg samples were separated by heavy-liquid and magnetic methods and then purified by hand picking under a binocular microscope. 1000 zircon grains were picked out from the samples, and 250 coarse zircon grains were selected to mount in epoxy resin discs. The mounts were polished until all zircon grains were cut in half. All grains were then photographed in transmitted, reflected light and Cathodoluminescence, in order to identify preferred locations for LA-MC-ICP-MS analysis.

U–Pb dating

Zircons were dated in situ on an excimer (213 nm wave length) laser ablation inductively coupled plasma mass spectrometer (LA-ICP-MS) at the Institute of Mineral Resources, China Academy of Geological Sciences. The GeoLas 2005 laser-ablation system was used for the laser ablation experiments. Helium was used as carrier gas to provide efficient aerosol transport to the ICP and minimize aerosol deposition around the ablation spot and within the transport tube. The used spot size was 30 μm, the used laser frequency was 10 Hz and the energy density is 2.5 J/cm^2. The laser ablation sampling used the single point ablation and we used the GJ-1 as external standard for U–Pb dating, M127 as the external standard for U and Th concentrations. We tested two GJ-1 and one Plesovice when 10 sample zircons have been tested, in order to observe instrument state and repeatability. The isotopic ratios were calculated using the ICPMSDataCal software (Liu *et al*., 2008) and the ages were calculated using ISOPLOT 3.0 (Ludwing, 2003). Our measurements of GJ-1 as an unknown sample yielded weighted ^{206}Pb/^{238}U ages of 600.3 ± 4.5 Ma, which is in good agreement with the apparent ID-TIMS ^{206}Pb/^{238}U ages of 598.5~602.7 Ma (Jackson *et al*., 2004). The measurements of Plesovice yielded weighted ^{206}Pb/^{238}U ages of 336.4 ± 2.2 Ma, which is also consistent with the apparent ID-TIMS ^{206}Pb/^{238}U ages of 337.13 ± 0.37 Ma (Sláma *et al*., 2008).

Lu–Hf isotopes

The Lu–Hf isotope analyses were done on a Nu Plasma HR MC-ICP-MS, coupled to a GeoLas 2005 excimer ArF laser ablation system hosted at the Institute of Mineral Resources, China Academy of Geological Sciences. The energy density used is 20 J/cm^2 and a spot size of 55 μm was used, Helium was also used as the carrier gas. The international standard zircon GJ-1 was used as reference material. The Hf isotopes were measured on the same spots or the same age domains with the concordant age determinations of grains, as guided by CL images. Analytical details for Lu–Hf isotope of zircons were reported in Hou and Yuan (2010). Our measured values of well-characterized zircon standards (GJ-1) yielded weighted ^{176}Hf/^{177}Hf ratios of 0.282015 ± 28 (2SD, n = 10), which agreed with the recommended values (Elhlou *et al*., 2006). The decay constant for ^{176}Lu and the CHUR ratios of ^{176}Hf/^{177}Hf and ^{176}Lu/^{177}Hf used in calculations are 1.867

Table 1. U–Pb isotopic compositions of detrital zircons of samples LH and LH2

Samples	Mass fraction (ppm)			Th/U	Isotopic ratio						Age (Ma)						Concordance (%)
	Pb	Th	U		$^{207}Pb/^{206}Pb$	1σ	$^{207}Pb/^{235}U$	1σ	$^{206}Pb/^{238}U$	1σ	$^{207}Pb/^{206}Pb$	1σ	$^{207}Pb/^{235}U$	1σ	$^{206}Pb/^{238}U$	1σ	
LH-01	381	483	218	2.21	0.0542	0.0003	0.2977	0.0023	0.0398	0.0002	389	15	265	2	252	1	95
LH-02	124	111	144	0.77	0.0508	0.0014	0.2310	0.0057	0.0330	0.0005	232	67	211	5	209	3	99
LH-03	5	19	25	0.79	0.0516	0.0045	0.2006	0.0175	0.0282	0.0010	333	202	186	15	179	6	96
LH-04	200	183	108	1.70	0.0557	0.0004	0.4077	0.0034	0.0531	0.0004	439	10	347	2	334	2	96
LH-05	11	35	32	1.09	0.0552	0.0023	0.3957	0.0194	0.0520	0.0010	420	99	339	14	327	6	96
LH-06	495	754	281	2.69	0.0525	0.0002	0.2297	0.0017	0.0318	0.0002	306	14	210	1	202	1	95
LH-07	194	187	97	1.93	0.0558	0.0003	0.3966	0.0042	0.0516	0.0005	443	13	339	3	324	3	95
LH-08	38	36	40	0.90	0.0528	0.0010	0.2452	0.0054	0.0337	0.0004	320	44	223	4	213	3	95
LH-09	133	19	22	0.86	0.1121	0.0006	4.7070	0.0743	0.3044	0.0046	1835	9	1768	13	1713	23	96
LH-10	25	7	7	1.03	0.1091	0.0022	4.3549	0.1396	0.2897	0.0095	1785	37	1704	26	1640	47	96
LH-100	50	43	31	1.42	0.0539	0.0017	0.2652	0.0069	0.0360	0.0006	365	68	239	6	228	3	95
LH-11	30	4	6	0.67	0.1130	0.0028	4.1082	0.1409	0.2654	0.0095	1848	44	1656	28	1518	48	91
LH-12	2614	334	237	1.41	0.1521	0.0007	9.2846	0.0813	0.4431	0.0043	2370	7	2366	8	2365	19	99
LH-13	66	41	40	1.02	0.0590	0.0023	0.3822	0.0138	0.0522	0.0043	565	85	329	10	328	26	99
LH-14	319	55	134	0.41	0.1089	0.0002	4.7093	0.0377	0.3142	0.0025	1781	3	1769	7	1761	12	99
LH-15	800	1047	1589	0.66	0.0496	0.0004	0.2615	0.0032	0.0383	0.0004	176	20	236	3	242	3	97
LH-16	759	94	100	0.94	0.1603	0.0003	10.1899	0.0742	0.4615	0.0032	2458	3	2452	7	2446	14	99
LH-17	96	143	106	1.35	0.0512	0.0020	0.1399	0.0026	0.0199	0.0011	250	86	133	2	127	7	95
LH-18	73	8	12	0.67	0.1685	0.0016	10.2886	0.1900	0.4424	0.0062	2543	15	2461	17	2362	28	95
LH-19	44	100	84	1.19	0.0527	0.0024	0.2247	0.0145	0.0309	0.0008	322	106	206	12	196	5	95
LH-20	406	74	143	0.52	0.1085	0.0002	4.6849	0.0318	0.3133	0.0020	1776	8	1765	6	1757	10	99
LH-21	962	180	189	0.95	0.1081	0.0004	4.5886	0.0351	0.3085	0.0028	1769	7	1747	6	1734	14	99
LH-22	84	126	52	2.43	0.0534	0.0010	0.2748	0.0048	0.0374	0.0004	346	43	247	4	237	2	96
LH-23	55	11	8	1.39	0.1121	0.0014	4.6011	0.1287	0.2973	0.0054	1835	22	1749	23	1678	27	95
LH-24	718	87	67	1.30	0.1646	0.0003	10.5144	0.0740	0.4638	0.0035	2503	2	2481	7	2456	15	98
LH-25	213	181	140	1.30	0.0563	0.0019	0.3522	0.0078	0.0454	0.0010	465	74	306	6	286	6	93
LH-26	106	79	53	1.48	0.0570	0.0004	0.4327	0.0036	0.0551	0.0003	500	13	365	3	346	2	94
LH-27	161	168	114	1.48	0.0555	0.0011	0.3716	0.0070	0.0486	0.0004	432	44	321	5	306	2	95
LH-28	95	117	117	0.99	0.0554	0.0003	0.2732	0.0021	0.0358	0.0002	428	11	245	2	227	1	92
LH-29	47	42	80	0.52	0.0541	0.0010	0.2880	0.0051	0.0387	0.0004	376	43	257	4	244	2	95
LH-30	4	18	20	0.88	0.0484	0.0066	0.2109	0.0220	0.0318	0.0009	120	293	194	18	202	6	96
LH-32	23	65	44	1.49	0.0512	0.0027	0.1707	0.0078	0.0243	0.0006	250	122	160	7	155	4	96
LH-33	18	22	15	1.46	0.0538	0.0015	0.2843	0.0076	0.0385	0.0005	365	66	254	6	244	3	95
LH-34	51	10	11	0.92	0.1107	0.0023	4.0929	0.1243	0.2678	0.0049	1813	38	1653	25	1530	25	92
LH-35	179	180	126	1.43	0.0516	0.0014	0.2507	0.0064	0.0353	0.0005	265	58	227	5	224	3	98
LH-36	74	103	83	1.24	0.0525	0.0016	0.2433	0.0058	0.0337	0.0006	309	75	221	5	214	4	96
LH-38	191	207	177	1.17	0.0517	0.0009	0.2540	0.0042	0.0356	0.0007	272	44	230	3	226	4	98
LH-39	4	3	4	0.87	0.0557	0.0026	0.4127	0.0194	0.0549	0.0016	443	97	351	14	344	10	98
LH-41	33	26	69	0.38	0.0543	0.0008	0.3031	0.0050	0.0405	0.0004	389	31	269	4	256	3	95
LH-42	402	474	1240	0.38	0.0530	0.0004	0.2650	0.0027	0.0362	0.0002	328	17	239	2	230	1	96
LH-43	570	940	400	2.35	0.0518	0.0004	0.1945	0.0015	0.0272	0.0002	276	19	180	1	173	1	95

Samples	Mass fraction (ppm)			Th/U	Isotopic ratio						Age (Ma)						Concordance (%)
	Pb	Th	U		$^{207}Pb/^{206}Pb$	1σ	$^{207}Pb/^{235}U$	1σ	$^{206}Pb/^{238}U$	1σ	$^{207}Pb/^{206}Pb$	1σ	$^{207}Pb/^{235}U$	1σ	$^{206}Pb/^{238}U$	1σ	
LH-44	118	22	16	1.37	0.1147	0.0016	4.1621	0.0590	0.2636	0.0048	1876	25	1667	12	1508	24	90
LH-45	102	122	414	0.29	0.0535	0.0002	0.2669	0.0019	0.0362	0.0002	350	12	240	2	229	2	95
LH-46	200	35	24	1.46	0.1292	0.0011	5.4015	0.0242	0.3031	0.0036	2087	15	1885	4	1707	18	90
LH-47	26	5	6	0.88	0.1136	0.0012	4.1633	0.0912	0.2664	0.0057	1858	19	1667	18	1522	29	90
LH-48	25	4	4	0.85	0.1114	0.0022	4.3646	0.1821	0.2842	0.0112	1833	36	1706	34	1613	56	94
LH-49	26	4	6	0.67	0.1136	0.0012	4.0622	0.0741	0.2601	0.0049	1858	19	1647	15	1491	25	90
LH-50	28	20	24	0.83	0.0526	0.0031	0.2172	0.0137	0.0299	0.0006	309	133	200	11	190	4	95
LH-51	36	5	7	0.69	0.1132	0.0008	4.0387	0.0584	0.2592	0.0036	1851	13	1642	12	1486	19	90
LH-52	33	40	36	1.13	0.0520	0.0019	0.2340	0.0097	0.0326	0.0007	283	83	214	8	207	5	96
LH-53	28	6	7	0.82	0.1161	0.0015	4.3025	0.1695	0.2689	0.0102	1898	23	1694	32	1535	52	90
LH-54	129	142	76	1.86	0.0559	0.0017	0.4361	0.0194	0.0566	0.0015	456	73	367	14	355	9	96
LH-55	146	25	99	0.25	0.1144	0.0010	4.9370	0.1103	0.3135	0.0086	1872	16	1809	19	1758	42	97
LH-56	115	209	100	2.09	0.0546	0.0007	0.2078	0.0044	0.0277	0.0005	394	31	192	4	176	3	91
LH-57	50	51	60	0.86	0.0565	0.0012	0.4212	0.0141	0.0541	0.0017	472	42	357	10	340	10	95
LH-58	29	29	12	2.47	0.0528	0.0017	0.3113	0.0128	0.0427	0.0012	320	68	275	10	269	7	97
LH-60	386	86	86	1.00	0.1115	0.0003	4.6102	0.0565	0.3000	0.0038	1824	6	1751	10	1691	19	96
LH-61	240	59	165	0.36	0.1058	0.0004	3.6042	0.0477	0.2472	0.0034	1728	40	1550	11	1424	18	91
LH-62	13	21	24	0.87	0.0533	0.0013	0.2275	0.0056	0.0312	0.0005	339	56	208	5	198	3	95
LH-63	48	123	55	2.26	0.0529	0.0010	0.2395	0.0118	0.0327	0.0013	324	43	218	10	207	8	95
LH-64	80	127	62	2.06	0.0542	0.0005	0.2611	0.0038	0.0350	0.0005	389	19	236	3	222	3	94
LH-65	358	73	43	1.69	0.1160	0.0003	4.9625	0.0566	0.3105	0.0036	1896	5	1813	10	1743	18	96
LH-66	4	17	8	2.14	0.0566	0.0067	0.3010	0.0330	0.0391	0.0023	476	265	267	26	247	14	92
LH-67	17	24	20	1.20	0.0910	0.0111	0.5026	0.1200	0.0315	0.0016	1456	234	413	81	200	10	30
LH-68	8	20	24	0.81	0.0525	0.0013	0.2056	0.0051	0.0286	0.0004	306	53	190	4	182	3	95
LH-69	15	4	5	0.87	0.1126	0.0012	4.7204	0.1121	0.3040	0.0062	1843	14	1771	20	1711	31	96
LH-70	364	51	46	1.11	0.1625	0.0005	10.0252	0.0629	0.4476	0.0030	2483	5	2437	6	2385	13	97
LH-71	115	25	30	0.84	0.1114	0.0010	4.2699	0.0593	0.2779	0.0029	1833	16	1688	11	1581	15	93
LH-73	13	5	6	0.75	0.1104	0.0026	4.0016	0.1326	0.2634	0.0079	1806	42	1635	27	1507	40	91
LH-74	43	82	109	0.75	0.0537	0.0004	0.2157	0.0020	0.0291	0.0002	361	17	198	2	185	1	93
LH-75	105	92	75	1.23	0.0593	0.0011	0.4918	0.0137	0.0600	0.0009	589	41	406	9	376	6	92
LH-77	10	52	71	0.73	0.0500	0.0018	0.2018	0.0055	0.0293	0.0005	198	79	187	5	186	3	99
LH-78	6	4	4	0.83	0.1118	0.0012	4.6988	0.1401	0.3050	0.0085	1829	21	1767	25	1716	42	97
LH-79	20	4	5	0.83	0.1138	0.0010	4.3231	0.0830	0.2762	0.0050	1861	17	1698	16	1572	25	92
LH-80	50	70	57	1.22	0.0569	0.0008	0.4504	0.0091	0.0574	0.0011	487	33	378	6	360	6	95
LH-81	333	64	117	0.54	0.1131	0.0003	4.9839	0.0425	0.3195	0.0026	1850	5	1817	7	1787	13	98
LH-82	91	89	97	0.91	0.0536	0.0011	0.2667	0.0131	0.0361	0.0016	354	44	240	10	228	10	95
LH-83	56	53	30	1.79	0.0565	0.0005	0.3600	0.0041	0.0463	0.0004	472	23	312	3	292	3	93
LH-84	84	79	65	1.21	0.0553	0.0007	0.3766	0.0059	0.0495	0.0006	433	28	325	4	312	4	95
LH-85	5	11	15	0.73	0.0529	0.0009	0.2170	0.0041	0.0299	0.0003	324	41	199	3	190	2	95
LH-86	375	415	398	1.04	0.0539	0.0002	0.2876	0.0021	0.0387	0.0003	369	7	257	2	245	2	95
LH-87	100	14	15	0.98	0.1121	0.0007	4.7291	0.0665	0.3061	0.0042	1835	7	1772	12	1721	21	97

Table 1. (continued)

Samples	Mass fraction (ppm)			Th/U	Isotopic ratio						Age (Ma)						Concordance (%)
	Pb	Th	U		$^{207}Pb/^{206}Pb$	1σ	$^{207}Pb/^{235}U$	1σ	$^{206}Pb/^{238}U$	1σ	$^{207}Pb/^{206}Pb$	1σ	$^{207}Pb/^{235}U$	1σ	$^{206}Pb/^{238}U$	1σ	
LH-88	54	28	49	0.58	0.0533	0.0018	0.2431	0.0094	0.0332	0.0014	343	76	221	8	210	9	95
LH-89	1938	183	260	0.70	0.1579	0.0005	9.7724	0.0911	0.4489	0.0039	2433	6	2414	9	2390	18	99
LH-90	202	25	16	1.58	0.1192	0.0011	4.8161	0.0745	0.2933	0.0046	1946	17	1788	13	1658	23	92
LH-91	72	9	12	0.73	0.1216	0.0017	5.1340	0.2143	0.3056	0.0100	1980	25	1842	35	1719	49	93
LH-92	17	4	7	0.66	0.1133	0.0015	4.6293	0.1161	0.2970	0.0070	1854	25	1755	21	1676	35	95
LH-93	46	54	28	1.96	0.0541	0.0011	0.2872	0.0065	0.0386	0.0005	372	46	256	5	244	3	95
LH-94	92	9	10	0.87	0.1129	0.0009	4.2585	0.0513	0.2736	0.0025	1847	15	1685	10	1559	12	92
LH-95	49	8	9	0.90	0.1135	0.0014	4.5211	0.0923	0.2892	0.0058	1857	23	1735	17	1637	29	94
LH-96	53	28	51	0.55	0.0561	0.0010	0.3723	0.0052	0.0482	0.0006	457	41	321	4	304	4	94
LH-97	57	9	9	1.06	0.1142	0.0008	4.4030	0.0499	0.2799	0.0028	1933	13	1713	9	1591	14	92
LH-98	378	41	29	1.38	0.1713	0.0004	10.8347	0.0767	0.4587	0.0031	2572	5	2509	7	2434	14	96
LH-99	38	50	27	1.85	0.0524	0.0034	0.2218	0.0083	0.0311	0.0012	306	153	203	7	198	8	97
LH2-01	254	184	251	0.73	0.0538	0.0003	0.2840	0.0038	0.0383	0.0004	361	13	254	3	242	2	95
LH2-02	542	51	29	1.75	0.1536	0.0007	8.3691	0.0985	0.3956	0.0043	2387	7	2272	11	2149	20	94
LH2-03	408	38	40	0.94	0.1694	0.0003	10.2811	0.0706	0.4411	0.0029	2552	2	2460	6	2355	13	95
LH2-04	125	50	41	1.21	0.0521	0.0027	0.2778	0.0028	0.0389	0.0016	300	149	249	2	246	10	98
LH2-05	553	521	189	2.76	0.0566	0.0001	0.3185	0.0010	0.0409	0.0001	476	4	281	1	258	1	91
LH2-06	634	60	29	2.09	0.1741	0.0006	10.3667	0.0769	0.4328	0.0033	2598	6	2468	7	2318	15	93
LH2-07	74	83	80	1.03	0.0529	0.0014	0.2582	0.0034	0.0355	0.0005	324	61	233	3	225	3	96
LH2-08	109	139	148	0.94	0.0540	0.0004	0.2850	0.0090	0.0384	0.0011	369	15	255	7	243	7	95
LH2-09	38	51	37	1.37	0.0507	0.0007	0.2005	0.0078	0.0287	0.0007	233	33	186	7	183	4	98
LH2-11	218	377	330	1.14	0.0528	0.0005	0.1408	0.0015	0.0193	0.0001	320	20	134	1	124	1	92
LH2-12	69	53	27	1.97	0.0529	0.0016	0.3198	0.0146	0.0438	0.0010	324	67	282	11	277	6	98
LH2-13	147	20	12	1.60	0.1167	0.0006	4.7116	0.0383	0.2930	0.0025	1906	9	1769	7	1656	13	93
LH2-14	171	192	98	1.96	0.0559	0.0015	0.2434	0.0064	0.0316	0.0003	450	61	221	5	200	2	90
LH2-15	25	31	27	1.14	0.0525	0.0014	0.2088	0.0059	0.0288	0.0003	309	56	193	5	183	2	95
LH2-16	12	45	48	0.95	0.0562	0.0028	0.4387	0.0145	0.0567	0.0010	461	111	369	10	355	6	96
LH2-17	640	69	49	1.41	0.1190	0.0004	5.4530	0.0311	0.3324	0.0017	1943	6	1893	5	1850	8	97
LH2-18	118	64	76	0.84	0.0583	0.0016	0.4675	0.0166	0.0582	0.0008	539	62	389	11	365	5	93
LH2-19	545	68	63	1.09	0.1154	0.0003	4.3112	0.0263	0.2709	0.0015	1887	4	1696	5	1545	8	90
LH2-20	66	61	114	0.54	0.0551	0.0014	0.2761	0.0063	0.0363	0.0002	417	53	248	5	230	1	92
LH2-21	286	25	39	0.63	0.1542	0.0006	8.6697	0.0929	0.4070	0.0033	2394	6	2304	10	2201	15	95
LH2-22	76	27	16	1.65	0.0578	0.0025	0.5176	0.0341	0.0649	0.0015	520	91	424	23	405	9	95
LH2-23	623	77	87	0.88	0.1149	0.0002	5.0434	0.1001	0.3182	0.0061	1877	3	1827	17	1781	30	97
LH2-24	400	44	32	1.39	0.1215	0.0006	5.4261	0.0392	0.3239	0.0021	1989	9	1889	6	1809	10	95
LH2-25	168	17	20	0.85	0.1155	0.0006	4.6417	0.0337	0.2916	0.0017	1887	10	1757	6	1650	9	93
LH2-26	130	15	14	1.09	0.1155	0.0010	4.4881	0.0688	0.2819	0.0040	1888	15	1729	13	1601	20	92
LH2-27	105	15	45	0.33	0.1111	0.0012	4.4336	0.1204	0.2895	0.0066	1817	19	1719	22	1639	33	95
LH2-28	470	43	28	1.54	0.1705	0.0005	10.3009	0.0939	0.4384	0.0041	2562	6	2462	8	2344	19	95
LH2-29	110	87	38	2.30	0.0529	0.0025	0.2339	0.0081	0.0323	0.0009	328	106	213	7	205	6	95
LH2-30	1426	219	129	1.70	0.1079	0.0005	4.1622	0.0806	0.2799	0.0060	1765	9	1667	16	1591	30	95

Samples	Mass fraction (ppm)			Th/U	Isotopic ratio						Age (Ma)						Concordance (%)
	Pb	Th	U		$^{207}Pb/^{206}Pb$	1σ	$^{207}Pb/^{235}U$	1σ	$^{206}Pb/^{238}U$	1σ	$^{207}Pb/^{206}Pb$	1σ	$^{207}Pb/^{235}U$	1σ	$^{206}Pb/^{238}U$	1σ	
LH2-31	137	19	15	1.25	0.1160	0.0008	4.3650	0.1247	0.2730	0.0076	1895	13	1706	24	1556	39	90
LH2-32	114	14	11	1.22	0.1189	0.0045	4.6508	0.2309	0.2822	0.0046	1940	67	1758	42	1602	23	90
LH2-33	652	77	87	0.89	0.1380	0.0003	7.5968	0.0483	0.3998	0.0029	2202	4	2184	6	2168	13	99
LH2-34	80	77	77	1.00	0.0531	0.0003	0.2719	0.0066	0.0371	0.0010	345	13	244	5	235	6	96
LH2-35	508	54	82	0.66	0.1647	0.0003	10.6896	0.0837	0.4707	0.0036	2505	4	2497	7	2487	16	99
LH2-36	409	56	177	0.32	0.1228	0.0008	5.8378	0.0843	0.3441	0.0035	1998	11	1952	13	1906	17	97
LH2-37	224	34	56	0.61	0.1169	0.0003	4.9784	0.0407	0.3091	0.0025	1909	4	1816	7	1736	12	95
LH2-38	240	37	51	0.72	0.1226	0.0003	5.6584	0.0480	0.3348	0.0028	1995	4	1925	7	1862	13	96
LH2-39	3	16	15	1.09	0.0554	0.0046	0.3434	0.0282	0.0453	0.0032	432	187	300	21	286	20	95
LH2-40	392	47	38	1.23	0.1729	0.0004	11.3484	0.1176	0.4765	0.0052	2587	4	2552	10	2512	23	98
LH2-41	517	504	225	2.25	0.0554	0.0006	0.3596	0.0052	0.0471	0.0005	428	–6	312	4	297	3	94
LH2-42	456	66	140	0.47	0.1164	0.0002	5.6361	0.0417	0.3515	0.0027	1902	4	1922	6	1942	13	98
LH2-44	449	44	132	0.33	0.1653	0.0008	10.3845	0.0972	0.4572	0.0050	2511	9	2470	9	2427	22	98
LH2-45	25	14	26	0.54	0.0515	0.0019	0.2092	0.0091	0.0295	0.0009	265	79	193	8	187	6	97
LH2-46	95	115	106	1.09	0.0511	0.0010	0.2655	0.0086	0.0377	0.0009	256	44	239	7	238	6	99
LH2-47	319	45	163	0.28	0.1095	0.0003	4.3754	0.0594	0.2900	0.0044	1792	6	1708	11	1641	22	96
LH2-48	224	26	149	0.17	0.1126	0.0002	4.9973	0.0919	0.3222	0.0062	1843	4	1819	16	1800	30	98
LH2-49	367	42	144	0.29	0.1112	0.0002	4.9794	0.0537	0.3252	0.0036	1818	2	1816	9	1815	17	99
LH2-50	80	100	91	1.11	0.0530	0.0014	0.1358	0.0040	0.0186	0.0004	332	27	129	4	119	3	91
LH2-51	134	258	220	1.17	0.0539	0.0012	0.1523	0.0088	0.0205	0.0007	369	50	144	8	131	5	90
LH2-52	120	111	107	1.04	0.0543	0.0016	0.2231	0.0119	0.0300	0.0022	383	69	205	10	190	14	92
LH2-53	173	21	65	0.32	0.1197	0.0005	5.6207	0.1145	0.3413	0.0075	1952	6	1919	18	1893	36	98
LH2-54	49	61	43	1.42	0.0532	0.0011	0.2643	0.0140	0.0360	0.0017	345	42	238	11	228	11	95
LH2-55	89	52	41	1.26	0.0576	0.0010	0.4045	0.0144	0.0509	0.0015	522	37	345	10	320	9	92
LH2-56	25	25	31	0.80	0.0537	0.0020	0.2848	0.0176	0.0383	0.0015	367	81	254	14	242	9	95
LH2-57	79	107	155	0.69	0.0544	0.0026	0.3260	0.0149	0.0437	0.0041	387	110	287	11	275	25	96
LH2-58	52	37	72	0.51	0.0561	0.0008	0.2461	0.0073	0.0319	0.0012	454	27	223	6	203	7	90
LH2-59	14	15	24	0.62	0.0560	0.0019	0.3592	0.0143	0.0465	0.0012	454	74	312	11	293	7	93
LH2-60	55	10	7	1.34	0.1288	0.0009	5.3584	0.1125	0.3017	0.0059	2081	13	1878	18	1700	29	90
LH2-61	0	15	16	0.95	0.0559	0.0023	0.2552	0.0117	0.0332	0.0009	456	93	231	9	210	6	90
LH2-62	37	57	80	0.71	0.0570	0.0025	0.3212	0.0160	0.0411	0.0033	500	96	283	12	260	20	91
LH2-63	38	63	72	0.87	0.0523	0.0049	0.1425	0.0162	0.0197	0.0004	298	210	135	14	126	3	92
LH2-64	65	71	65	1.08	0.0563	0.0029	0.2814	0.0286	0.0360	0.0020	465	113	252	23	228	12	90
LH2-65	50	42	43	0.97	0.0567	0.0010	0.3008	0.0082	0.0386	0.0010	480	41	267	6	244	6	90
LH2-66	106	14	9	1.67	0.1291	0.0014	5.6158	0.3125	0.3154	0.0172	2087	14	1919	48	1767	84	91
LH2-67	67	67	54	1.24	0.0567	0.0007	0.3532	0.0189	0.0452	0.0028	480	28	307	14	285	17	92
LH2-68	175	178	121	1.48	0.0544	0.0011	0.2760	0.0144	0.0368	0.0027	391	46	247	11	233	17	94
LH2-69	91	91	40	2.28	0.0560	0.0012	0.2850	0.0168	0.0370	0.0021	450	16	255	13	234	13	91
LH2-70	53	56	56	1.00	0.0556	0.0011	0.2821	0.0054	0.0369	0.0010	435	44	252	4	234	6	92
LH2-71	223	137	138	1.00	0.0573	0.0012	0.3399	0.0125	0.0430	0.0009	502	44	297	9	271	6	90
LH2-72	64	49	54	0.91	0.0601	0.0004	0.4612	0.0022	0.0557	0.0005	606	15	385	2	349	3	90

Table 1. (continued)

Samples	Mass fraction (ppm)			Th/U	Isotopic ratio						Age (Ma)						Concordance (%)
	Pb	Th	U		$^{207}Pb/^{206}Pb$	1σ	$^{207}Pb/^{235}U$	1σ	$^{206}Pb/^{238}U$	1σ	$^{207}Pb/^{206}Pb$	1σ	$^{207}Pb/^{235}U$	1σ	$^{206}Pb/^{238}U$	1σ	
LH2-73	136	86	56	1.54	0.0591	0.0007	0.4435	0.0056	0.0544	0.0004	572	26	373	4	342	2	91
LH2-74	56	43	32	1.36	0.0542	0.0011	0.2635	0.0049	0.0354	0.0005	389	51	238	4	224	3	94
LH2-75	510	52	40	1.29	0.1702	0.0005	9.3882	0.0713	0.3998	0.0024	2561	5	2377	7	2168	11	90
LH2-76	183	197	217	0.91	0.0551	0.0003	0.2531	0.0024	0.0333	0.0003	417	11	229	2	211	2	91
LH2-77	336	41	78	0.53	0.1193	0.0002	5.3207	0.0380	0.3235	0.0022	1946	4	1872	6	1807	11	96
LH2-78	268	28	38	0.74	0.1525	0.0006	7.5085	0.1348	0.3572	0.0060	2374	6	2174	16	1969	29	90
LH2-79	97	76	67	1.14	0.0553	0.0030	0.2795	0.0176	0.0367	0.0012	433	122	250	14	232	7	92
LH2-80	116	72	63	1.13	0.0581	0.0007	0.3919	0.0063	0.0489	0.0006	600	29	336	5	308	3	91
LH2-81	660	65	81	0.80	0.1637	0.0003	9.9017	0.0628	0.4392	0.0028	2494	4	2426	6	2347	13	96
LH2-82	428	64	48	1.32	0.1136	0.0005	4.4306	0.0430	0.2831	0.0025	1858	8	1718	8	1607	12	93
LH2-83	254	37	63	0.58	0.1158	0.0007	4.3446	0.0955	0.2722	0.0056	1892	10	1702	18	1552	28	90
LH2-84	26	34	34	1.00	0.0509	0.0010	0.2102	0.0037	0.0300	0.0006	239	46	194	3	190	4	98
LH2-85	75	58	24	2.42	0.0558	0.0032	0.2640	0.0211	0.0342	0.0008	456	123	238	17	217	5	90
LH2-86	29	37	41	0.90	0.0514	0.0020	0.1315	0.0036	0.0187	0.0004	257	87	125	3	120	3	95
LH2-87	47	5	7	0.77	0.1131	0.0013	4.5885	0.1111	0.2947	0.0086	1850	21	1747	20	1665	43	95
LH2-88	810	86	26	3.30	0.1724	0.0005	10.5520	0.1195	0.4441	0.0046	2581	6	2485	11	2369	20	95
LH2-89	0	11	14	0.81	0.0524	0.0027	0.2131	0.0035	0.0299	0.0018	302	114	196	3	190	11	96
LH2-90	29	23	24	0.96	0.0550	0.0011	0.3695	0.0082	0.0488	0.0007	413	46	319	6	307	5	96
LH2-91	196	30	72	0.42	0.1245	0.0003	5.6212	0.0338	0.3276	0.0020	2022	5	1919	5	1827	10	95
LH2-92	30	45	91	0.50	0.0552	0.0005	0.2334	0.0027	0.0307	0.0003	420	−14	213	2	195	2	91
LH2-93	113	151	100	1.51	0.0552	0.0004	0.2833	0.0030	0.0372	0.0004	420	15	253	2	236	2	92
LH2-94	152	29	44	0.65	0.1231	0.0003	5.1028	0.0353	0.3006	0.0021	2002	4	1837	6	1694	10	91
LH2-95	174	37	131	0.28	0.1096	0.0007	3.9244	0.0762	0.2599	0.0057	1794	12	1619	16	1489	29	91
LH2-96	105	227	172	1.32	0.0549	0.0005	0.2346	0.0042	0.0310	0.0005	409	22	214	3	197	3	91

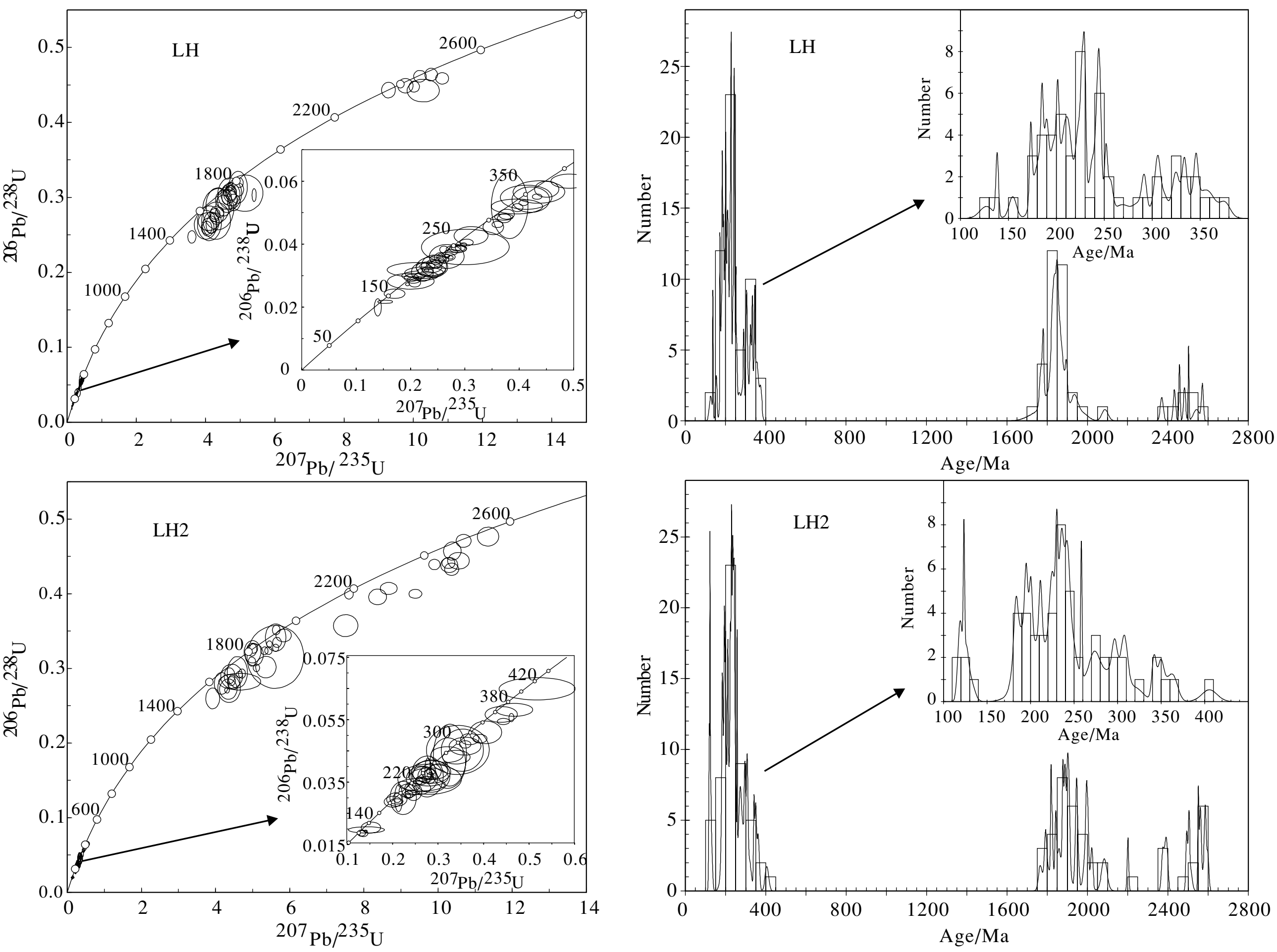

Fig. 2. Concordance and distribution diagrams of U–Pb ages from samples of LH and LH2.

× 10^{-11} (Scherer *et al.*, 2001) and 0.282772 and 0.0332 (Blichert-Toft and Albarède, 1997), respectively. The two-stage model age (T_{DM2}) was calculated relative to the depleted mantle with a present-day $^{176}Hf/^{177}Hf$ = 0.28325 and $^{176}Lu/^{177}Hf$ = 0.0384 (Griffin *et al.*, 2000), and the $^{176}Lu/^{177}Hf$ of continental crust is 0.015 (Blichert-Toft and Albarède, 1997; Griffin *et al.*, 2000; Geng *et al.*, 2012; Diwu *et al.*, 2012).

RESULTS

In this paper, 99 and 96 zircon grains from samples LH and LH2 was analyzed by LA-MC-ICP-MS, respectively. 94 and 95 zircon grains yielded concordant ages (with age concordance in the range from 90% to 110%) in the samples LH and LH2 (Table 1), respectively. According to zircon U–Pb concordant ages, 27 zircons from sample LH and 38 zircons from sample LH2 were selected to determine Lu–Hf isotopic compositions. The following results and discussions are based on the concordant zircons, and we used $^{207}Pb/^{206}Pb$ ages for zircons of age ≥1,000 Ma and $^{206}Pb/^{238}U$ ages for zircons of age <1,000 Ma (Yang *et al.*, 2009).

U–Pb ages

The concordant zircons from sample LH show three major age populations of 2370 Ma~2572 Ma, 1728~2087 Ma and 127~376 Ma and the concordant zircons from sample LH2 also yield three major age populations of 2374~2598 Ma, 1765~2087 Ma and 119~405 Ma (Fig. 2). In sample LH, the ages populations of 2370 Ma~2572 Ma, 1728~2087 Ma and 127~376 Ma account for 8%, 34% and 58%, respectively. In sample LH2, the ages populations of 2374~2598 Ma, 1765~2087 Ma and 119~405 Ma account for 13%, 31% and 56%, respectively. The concordant zircons from the two samples of LH and LH2 show broadly similar age patterns with age populations and proportions. Meanwhile, samples LH and LH2 have a common feature that there is not concordant zircons with ages of 500~1700 Ma.

Table 2. Lu–Hf isotopic compositions of detrital zircons of samples LH and LH2

Sample	U–Pb age (Ma)	$^{176}Lu/^{177}Hf$	2σ	$^{176}Hf/^{177}Hf$	2σ	$\varepsilon_{Hf}(t)$	T_{DM2}	2σ
LH-01	252	0.001282	0.000013	0.28234	0.00002	–10.0	1905	±44
LH-03	179	0.001014	0.000006	0.28241	0.00002	–9.1	1794	±51
LH-08	213	0.001297	0.000014	0.28253	0.00002	–4.0	1497	±49
LH-09	1835	0.001091	0.000011	0.28152	0.00002	–4.9	2786	±44
LH-10	1785	0.000400	0.000003	0.28151	0.00002	–5.5	2784	±46
LH-14	1781	0.000910	0.000018	0.28149	0.00002	–6.7	2854	±45
LH-16	2458	0.000742	0.000005	0.28128	0.00002	1.2	2894	±38
LH-21	1769	0.000770	0.000007	0.28152	0.00002	–5.9	2801	±44
LH-22	237	0.000723	0.000003	0.28228	0.00002	–12.3	2038	±46
LH-26	346	0.000581	0.000002	0.28199	0.00002	–20.3	2611	±52
LH-34	1813	0.000911	0.000009	0.28152	0.00003	–4.8	2767	±56
LH-36	214	0.001997	0.000131	0.28250	0.00003	–5.2	1571	±64
LH-38	226	0.000890	0.000004	0.28230	0.00002	–11.7	1992	±41
LH-53	1898	0.000519	0.000009	0.28148	0.00002	–4.0	2783	±52
LH-55	1872	0.000746	0.000029	0.28154	0.00002	–2.6	2675	±36
LH-58	269	0.000372	0.000001	0.28214	0.00002	–16.5	2323	±40
LH-60	1824	0.000118	0.000001	0.28158	0.00002	–1.6	2577	±35
LH-66	247	0.000806	0.000008	0.28187	0.00002	–26.7	2933	±46
LH-69	1843	0.000541	0.000004	0.28153	0.00002	–3.5	2709	±40
LH-79	1861	0.000464	0.000003	0.28149	0.00002	–4.4	2779	±54
LH-81	1850	0.000860	0.000022	0.28149	0.00002	–5.2	2816	±44
LH-83	292	0.001314	0.000043	0.28261	0.00004	0.6	1269	±79
LH-92	1854	0.000561	0.000010	0.28152	0.00003	–3.8	2734	±60
LH-96	304	0.000162	0.000007	0.28238	0.00004	–7.2	1768	±96
LH-98	2572	0.000556	0.000002	0.28126	0.00003	3.2	2858	±66
LH-99	198	0.000807	0.000006	0.28204	0.00003	–21.7	2590	±62
LH-100	228	0.000783	0.000008	0.28218	0.00003	–16.2	2270	±55
LH2-03	2552	0.000832	0.000005	0.28131	0.00002	4.2	2783	±43
LH2-1	242	0.002164	0.000004	0.28218	0.00003	–16.0	2271	±55
LH2-4	246	0.002021	0.000007	0.28245	0.00003	–6.5	1678	±61
LH2-7	225	0.000666	0.000007	0.28278	0.00002	5.2	927	±54
LH2-9	183	0.001827	0.000010	0.28255	0.00003	–3.9	1468	±65
LH2-11	124	0.001203	0.000008	0.28247	0.00002	–8.1	1689	±49

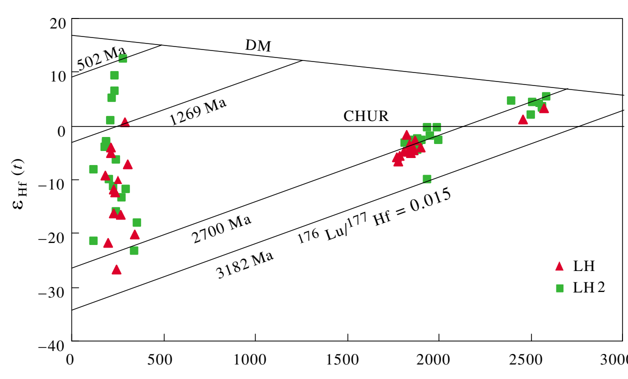

Fig. 3. U–Pb age versus $\varepsilon_{Hf}(t)$ value plots of concordant detrital zircons from LH and LH2.

Lu–Hf isotopes

As shown in Fig. 3, the $\varepsilon_{\mathrm{Hf}}(t)$ values of sample LH yield a wide range from –26.7 to 3.2, and the $\varepsilon_{\mathrm{Hf}}(t)$ values of sample LH2 exhibit a more wide range from –23.4 to 12.6 (Table 2). Samples LH and LH2 have a similar $\varepsilon_{\mathrm{Hf}}(t)$ values except for four concordant zircons with ages of ~250 Ma. Figure 3 can also shows the distribution of the Hf continental model ages (T_{DM2}). Zircons, which show age populations of ~2.5 Ga and 1.8 Ga in samples LH and LH2, have approximate T_{DM2} values of 2.7 Ga. But four detrital zircons with ages of ~250 Ma in sample LH2 have a different character that $T_{DM2} < 1000$ Ma and $\varepsilon_{\mathrm{Hf}}(t) > 0$. According to the geological setting, the Kerqin sandy land has the zircons with U–Pb ages at ~250 Ma and $T_{DM2} < 1000$ Ma (Xie *et al.*, 2007), which is the material from the Xing-Meng Orogenic Belt (Kuzmichev *et al.*, 2005; Demoux *et al.*, 2009). So we must delete these data when calculated continental crust growth rate of the North China Craton.

Discussion

Provenance of floodplain sediments

The Laoha River drains entirely within the North China Craton. Detrital zircons from upper and lower

Table 2. (continued)

Sample	U–Pb age (Ma)	$^{176}Lu/^{177}Hf$	2σ	$^{176}Hf/^{177}Hf$	2σ	$\varepsilon_{Hf}(t)$	T_{DM2}	2σ
LH2-13	1906	0.000583	0.000025	0.28151	0.00002	–2.7	2708	±42
LH2-16	355	0.000925	0.000013	0.28205	0.00002	–18.0	2476	±46
LH2-17	1943	0.000346	0.000003	0.28128	0.00002	–10.0	3183	±41
LH2-19	1887	0.000418	0.000002	0.28147	0.00002	–4.6	2809	±43
LH2-21	2394	0.001367	0.000006	0.28144	0.00002	4.5	2641	±46
LH2-25	1887	0.000599	0.000001	0.28154	0.00002	–2.4	2674	±42
LH2-26	1888	0.001096	0.000045	0.28155	0.00002	–2.6	2686	±41
LH2-27	1817	0.000552	0.000006	0.28156	0.00002	–3.1	2667	±41
LH2-28	2562	0.001002	0.000012	0.28129	0.00002	3.5	2831	±47
LH2-29	205	0.001214	0.000005	0.28237	0.00003	–10.1	1872	±65
LH2-31	1895	0.000628	0.000011	0.28152	0.00002	–2.9	2712	±43
LH2-32	1940	0.000632	0.000009	0.28156	0.00002	–0.3	2587	±45
LH2-34	235	0.001501	0.000015	0.28281	0.00002	6.3	860	±50
LH2-35	2505	0.000790	0.000010	0.28128	0.00002	2.0	2880	±39
LH2-38	1995	0.000297	0.000001	0.28151	0.00002	–0.4	2634	±41
LH2-39	286	0.000818	0.000010	0.28295	0.00003	12.6	502	±61
LH2-40	2587	0.000396	0.000001	0.28130	0.00002	5.4	2735	±44
LH2-41	297	0.002520	0.000074	0.28226	0.00003	–11.9	2058	±73
LH2-44	2511	0.000137	0.000004	0.28131	0.00002	4.4	2737	±41
LH2-46	238	0.000515	0.000005	0.28289	0.00003	9.2	682	±63
LH2-48	1843	0.001301	0.000003	0.28157	0.00002	–2.9	2674	±40
LH2-53	1952	0.000511	0.000058	0.28151	0.00002	–1.9	2691	±43
LH2-54	228	0.001224	0.000016	0.28231	0.00003	–11.4	1972	±67
LH2-57	275	0.001831	0.000011	0.28223	0.00004	–13.4	2131	±78
LH2-73	342	0.000788	0.000003	0.28190	0.00003	–23.4	2799	±61
LH2-75	2561	0.000367	0.000011	0.28125	0.00002	3.2	2852	±40
LH2-76	211	0.001506	0.000010	0.28267	0.00003	1.0	1183	±66
LH2-82	1858	0.001791	0.000023	0.28158	0.00003	–2.8	2677	±63
LH2-84	190	0.003213	0.000008	0.28258	0.00005	–3.0	1415	±112
LH2-86	120	0.000985	0.000003	0.28209	0.00003	–21.6	2525	±64
LH2-89	190	0.001720	0.000013	0.28257	0.00005	–3.3	1438	±104
LH2-94	2002	0.000462	0.000001	0.28145	0.00002	–2.7	2782	±46

reaches of the Laoha River have the same age populations. They show prominent U–Pb age peaks at 2.4~2.5 Ga and 1.8~1.9 Ga, which are the characteristic of the North China Craton (Fig. 4A) (Wan *et al.*, 2000, 2006a, 2006b, 2010, 2012b; Kusky *et al.*, 2001; Li *et al.*, 2007). The 2.4~2.5 Ga ages are widespread in the North China Craton, which represents the strongest magmatic events in the North China Craton. In the northeast of North China Craton, the SHIRMP age of Zhangsangou Formation is 2517~2534 Ma (Li *et al.*, 2009); the basement rocks in the Anshan area have the ages of Neoarchean (Liu *et al.*, 2007). The 1.8~1.90 Ga age is an important period that represents the collision between the East and West blocks in the North China Craton (Wan *et al.*, 2000; Zhao *et al.*, 2000; Guan *et al.*, 2002; Guo *et al.*, 2005; Xia *et al.*, 2006; Liu *et al.*, 2011a, b; Liu, S. W. *et al.*, 2012; Li *et al.*, 2012; Santosh *et al.*, 2013). In the Lushan area of Henan province, the metamorphic rocks have 1.84~1.87 Ga ages (Wan *et al.*, 2006a). The 1.8–1.9 Ga zircons have also been found in the Paleoproterozoic Yejishan, Hutuo, Zhongtiao, Gantaohe and Songshan Groups in the Trans-North China Orogen (Liu *et al.*, 2011a, 2011b, 2012a, 2012b, 2012c). In the Daqingshan area in the Western Block of the North China Craton, the Precambrian Khondalite Belt recorded the ~1.9 Ga ages, which represent the metamorphic events of the North China Craton (Wan *et al.*, 2009; Zhao *et al.*, 2010). In the Eastern Block of the North China Craton, a large amount of 1.8–1.9 Ga zircons have been revealed in the Paleoproterozoic Jiao-Liao-Ji Belt (Li *et al.*, 2004, 2005, 2006; Luo *et al.*, 2004, 2008; Li and Zhao, 2007; Zhou *et al.*, 2008; Tam *et al.*, 2011, 2012a, 2012b, 2012c). After 1.7 Ga, the Precambrian basements of the North China Craton had been stabilized until the Ordovician (Gao *et al.*, 2002), which led to the lack of 500~1700 Ma detrital zircons in the Laoha River. In the Mesozoic (~130 Ma), the magmatic activity was very intense, leading to the reactivation of the North China Craton, but no zircon with two stage Hf crust model age of Mesozoic were found.

According to the T_{DM2} of the Laoha River, the strongest peak is 2.7 Ga, which is consistent with the northeast margin of the North China Craton (Fig. 4B) and the global continental crust (Kemp *et al.*, 2006; Hawkesworth *et al.*, 2010; Condie *et al.*, 2011). However, four detrital

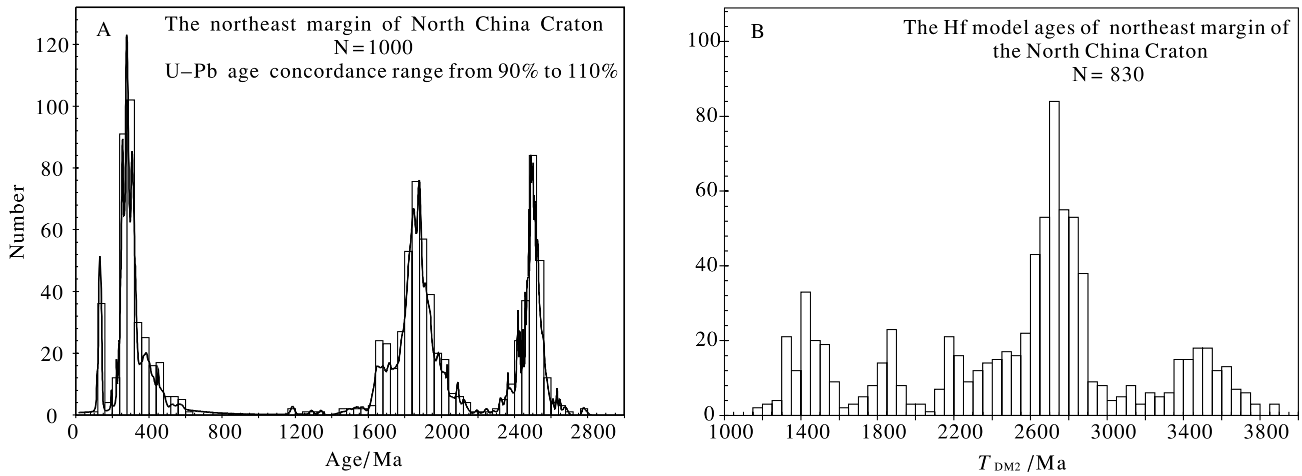

Fig. 4. U–Pb ages and Hf model ages of the northeast margin of North China Craton. Data from the published articles (Xia et al., 2006; Wu et al., 2007; Zhang, S. H. et al., 2007; Wan et al., 2008; Yang et al., 2009; Shi et al., 2010; Su et al., 2011; Wang et al., 2011; Zhang et al., 2011; Bao et al., 2012).

zircons from sample LH2 have the T_{DM2} ages of <1000 Ma. The northeast area of the Laoha River is the Kerqin sandy land, which has the detrital zircons from the Xing-Meng Orogeny Belt (Xie *et al*., 2007). Therefore, these four detrital zircons of LH2 are interpreted to have been sourced from the Xing-Meng Orogeny Belt.

Continental crustal evolution and growth of the northeast margin of the North China Craton

The dominant Nd crust model ages in the North China Craton range from 2.6~3.0 Ga and are older than 1.8 Ga (Wu *et al*., 2005). The strongest peak of Hf model ages in the North China Craton is ~2.7 Ga (Fig. 4B) (Yang *et al*., 2009; Geng *et al*., 2012; Diwu *et al*., 2012). In this paper, the dominant two stage Hf crust model ages is also 2.7 Ga and the detrital zircons with two stage Hf crust model ages younger than 1.8 Ga exist, which is consistent with the previous studies (Yang *et al*., 2009; Diwu *et al*., 2012). Therefore, the strongest growth period of continental crust in the northeast margin of North China Craton is ~2.7 Ga and the strongest magmatic events in the northeast margin of North China Craton is ~2.5 Ga, which indicates that the residence time in the detrital zircons with ages of ~2.5 Ga is ~200 Ma. The subordinate U–Pb ages peak of detrital zircons in the Laoha River is ~1.8 Ga and the two stage Hf crust model age of these detrital zircons is also ~2.7 Ga, which also indicates that the best estimation age of mantle extraction of the North China Craton is ~2.7 Ga. As discussed above, very few detrital zircons have $\varepsilon_{Hf}(t)$ values identical to depleted mantle values, which suggests the studied detrital zircons contain amounts of reworking crustal materials.

Yang *et al*. (2009) used two stage Hf crust model ages of detrital zircons in the Luan River and Yongding River

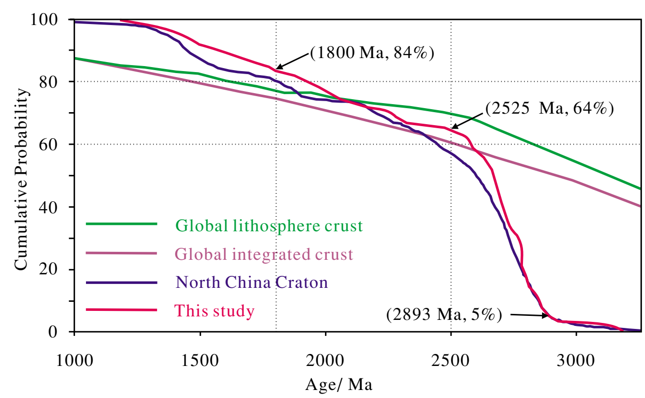

Fig. 5. Cumulative probability curve of detrital zircons in the Laoha River. The data of global lithosphere crust and global integrated crust quote by Belousova et al. (2010), the data of North China Craton quote by Xia et al. (2006), Zhang, S. H. et al. (2007), Wan et al. (2008), Yang et al. (2009), Shi et al. (2010), Zhang et al. (2011), Wang et al. (2011), Bao et al. (2012) and Diwu et al. (2012).

to study the continental crust growth of North China Craton. Crustal growth rates based on T_{DM2} suggested that 45% and 90% of the present crustal volume were formed by 2.5 Ga and 1.0 Ga, respectively. Geng *et al*. (2011) studied the detrital zircons from the Daqing River, Chaobai River and Liaohe River, and suggested that 80% of the present crustal volume in the east of North China Craton was formed by 2.2 Ga. Diwu *et al*. (2012) analyzed the U–Pb and Lu–Hf isotopes of 187 concordant detrital zircons form the Jing and Luo River in Shanxi Province, China, to constrain the evolution of the West Block of the North China Craton. About 60% of the present crustal volume in the North China Craton was generated in the between Mesoarchean and Late Neoarchean (3.0 to 2.5 Ga). Since then, the continental crust remains a stable rate of growth and completely formed at the end of the Neoproterozoic (600 Ma). On the other hand, the continental crust of the North China Craton that formed at 2.5 Ga is juvenile component, not reworking crust. In this paper, Fig. 5 shows that 5%, 64% and 84% of the present crustal volume were formed by 2893 Ma, 2525 Ma and 1800 Ma, respectively. 64% of the present crustal volume in the northeast margin of the North China Craton, which were formed by 2.5 Ga, is higher than the 45% from the whole North China Craton (Yang *et al*., 2009) and consistent with 60% from the Western Block of the North China Craton (Diwu *et al*., 2012) and global continental crust (Kemp *et al*., 2006; Hawkesworth *et al*., 2010; Belousova *et al*., 2010; Condie *et al*., 2011). It indicates that the continental crust growth of North China Craton is not uniform at 2.5 Ga, but the growth rate of the northeast margin of North China Craton is consistent with the Western Block of North China Craton and global continental crust. 84% of the present crustal volume in the northeast margin of North China Craton has been formed at 1.8 Ga. After that, the North China Craton has completed cratonization, indicating that the North China Carton could remain quiescent with zero to negligible growth. Figure 5 can also reveal that the continental growth of the northeast margin of North China Craton was an episodic growth, not continuous.

Recently, how to quantitatively estimate the growth rate of continental crust is an enigmatic issue (Iizuka *et al*., 2010; Dhuime *et al*., 2012). In this paper, the formulas, proposed by Iizuka *et al*. (2010) have been quoted to calculate the reworking rate of continental ctust. The formulas are expressed as the following equations:

$$\left[\frac{^{176}\mathrm{Hf}}{^{177}\mathrm{Hf}}\right]_{t_n}^{\mathrm{GC}} = \alpha_n \times \left[\frac{^{176}\mathrm{Hf}}{^{177}\mathrm{Hf}}\right]_{t_n}^{\mathrm{RC}} + (1-\alpha_n)\times\left[\frac{^{176}\mathrm{Hf}}{^{177}\mathrm{Hf}}\right]_{t_n}^{\mathrm{DM}} \quad (1)$$

$$\begin{aligned}\left[\frac{^{176}\mathrm{Hf}}{^{177}\mathrm{Hf}}\right]_{t_n}^{\mathrm{RC}} &= \sum_0^{n-1} a_i \times x \\ &\times\left[\left[\frac{^{176}\mathrm{Hf}}{^{177}\mathrm{Hf}}\right]_{t_n}^{\mathrm{GC}} + \left[\frac{^{176}\mathrm{Lu}}{^{177}\mathrm{Hf}}\right]^{\mathrm{granitoid}} \times \left(e^{\lambda(t_i-t_n)}-1\right)\right] \\ &+\sum_0^{n-1} a_i \times (1-x)\times \\ &\left[\left[\frac{^{176}\mathrm{Hf}}{^{177}\mathrm{Hf}}\right]_{t_i}^{\mathrm{DM}} + \left[\frac{^{176}\mathrm{Lu}}{^{177}\mathrm{Hf}}\right]^{\mathrm{mafic}} \times \left(e^{\lambda(t_i-t_n)}-1\right)\right] \quad (2)\end{aligned}$$

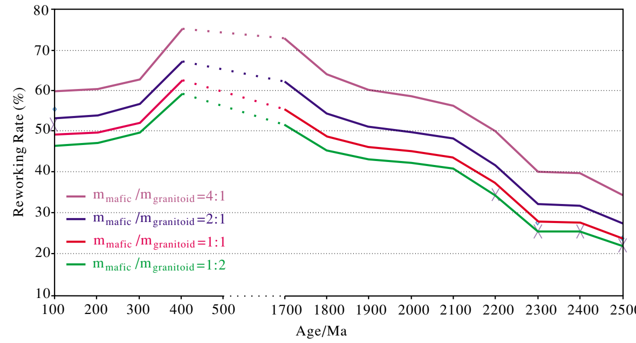

Fig. 6. Reworking rate as a function of time. After 1700 Ma, the North China Craton completed cratonization, which indicates the North China Carton could remain quiescent with zero to negligible growth, but reactivated after 500 Ma. Therefore, the North China Craton could remain quiescent with zero to negligible growth from 1700 Ma to 500 Ma, so we used the dotted lines to express it.

$$\begin{aligned}x &= \frac{m_{\mathrm{granitoid}} \times C_{\mathrm{granitoid}}^{\mathrm{Hf}}}{m_{\mathrm{granitoid}} \times C_{\mathrm{granitoid}}^{\mathrm{Hf}} + m_{\mathrm{mafic}} \times C_{\mathrm{mafic}}^{\mathrm{Hf}}} \\ &= \frac{1}{1+\left(m_{\mathrm{mafic}}/m_{\mathrm{granitoid}}\right)\times\left(C_{\mathrm{mafic}}^{\mathrm{Hf}}/C_{\mathrm{granitoid}}^{\mathrm{Hf}}\right)} \quad (3)\end{aligned}$$

$$\sum_0^{n-1} a_i = 1 \ (a_i \ge 0). \quad (4)$$

The initial Hf isotope ratio of the granitoid crust formed during the *n*th event at time t_n is calculated by formula (1). Where acronyms GC, RC and DM represent the granitoid crust, reworked crustal component and depleted mantle, respectively, and α is the reworking rate. The Hf isotope ratio of the reworking crust formed during the *n*th event at time t_n is calculated by formula (2), which is composed of two parts, granitoid and mafic rocks. x represents the ratio of $^{176}Hf/^{177}Hf$ between granitoid and mafic rocks, and it can be calculated by formula (3). $C_{granitoid}{}^{Hf}$ and $C_{mafic}{}^{Hf}$ are the concentrations of Hf in the granitoid and mafic rocks, respectively. The Hf contents of average precambrian granitoid crust (9.0 ppm; (Vervoort and Jonathan Patchett, 1996)) and of mafic lower crust (1.9 ppm; (Rudnick and Fountain, 1995)) were used for $C_{granitoid}{}^{Hf}$ and $C_{mafic}{}^{Hf}$. $m_{granitoid}$ and m_{mafic} are the mass of the granitoid and mafic rocks. Where a_i is the contribution of the pre-existing crust formed in the *i*th event to the reworked crustal component, which is from the percentage of T_{DM2}. In this paper, the mass ratio between mafic and granitoid is unknown during the early history of earth, 4:1, 2:1, 1:1 and 1:2 are assumed to used for the ratio of $m_{mafic}/m_{granitoid}$. λ_{Lu} = 1.867 × 10^{-11}

(Söderlund *et al.*, 2003), 0.015, 0.021 and 0.0384 (Griffin *et al.*, 2000) are used for the ratio of $[^{176}Lu/^{177}Hf]^{granitoid}$, $[^{176}Lu/^{177}Hf]^{mafic}$ and $[^{176}Lu/^{177}Hf]^{DM}$; 0.28147 (the average ratio of $^{176}Hf/^{177}Hf$ in this study) and 0.28325 (Griffin *et al.*, 2000) represent the ratio of $^{176}Hf/^{177}Hf$ in the average continental crust and depleted mantle, respectively. As no evidence for reworking of crust older than 3.2 Ga, our calculations start from 3200 Ma (i.e., t_0 = 3200 Ma). We have considered that crust formation events take place with a regular time interval of 100 Ma, and we used a time window with ±100 Ma.

In the North China Craton, the time of 2.5 Ga is the period of strongest magmatic events (Li *et al.*, 2009; Liu *et al.*, 2007; Shen *et al.*, 2005; Lu *et al.*, 2008; Yang *et al.*, 2008; Zhao *et al.*, 2011; Wu *et al.*, 2013), and the T_{DM2} of rocks with ages of 2.5 Ga is mainly 2.7 Ga. In traditional views, the rocks with ages of 2.5 Ga are considered to be the reworked products of the ~2.7 Ga crusts. However, the North China Craton had a low reworking rate at 2.5 Ga (Fig. 6), which indicates the time of 2.5 Ga is also the main growth period in the North China Craton (Diwu *et al.*, 2012). The reworking rates gradually increased with the decreasing of age in the Precambrian and the reworking rate is close to 0.5 at ~1.8 Ga, which indicates that the continental crust of the North China Craton is composed mainly of the juvenile crust during Precambrian times. From 400 Ma to 100 Ma, the reworking rates droped gradually, but the ratio between juvenile and reworking crust was still very low, which is consistent with the reactivation of the North China Craton (Gao *et al.*, 2002; Wu *et al.*, 2003; Zheng *et al.*, 2005).

Over all, the strongest continental crust growth of the North China Craton occurred at 2.5 Ga and 2.7 Ga. The strongest reworking period in the North China Craton is at 1.8 Ga, and the North China Craton still maintained a high ratio between reworking and juvenile crusts after reactivating, but the addition of juvenile crust was gradually increased.

Conclusions

(1) U–Pb ages of detrital zircons in the samples of LH and LH2 reveal three major age groups of 2370 Ma~2572 Ma, 1728~2087 Ma, 127~376 Ma and 2374~2598 Ma, 1765~2087 Ma, 119~405 Ma, respectively, which indicates the prominent magmatic events at ~1.8 Ga and ~2.5 Ga.

(2) Samples LH and LH2 have the common prominent two stage Hf model ages with a peak at 2.7 Ga, which suggests the best estimation age of mantle extraction of the northeast margin of North China Craton is 2.7 Ga. Detrital zircons with U–Pb ages of ~1.8 Ga and ~2.5 Ga have the two stage Hf crust model ages of 2.7 Ga, and very few detrital zircons have $\varepsilon_{Hf}(t)$ values identical to depleted mantle values. These indicate that the majority of continental crust of the northeast margin of the North China Craton originated from reworking crust with age of ~2.7 Ga.

(3) The continental crust volume of the North China Craton began to increase fleetly from 2.9 Ga to 1.8 Ga. About 5% of the present crustal volume in the northeast margin of North China Craton was formed at 2.9 Ga; whereas ~64% of the present crustal volume in the northeast margin of North China Craton has formed at 2.5 Ga, which is consistent with the Western Block of the North China Craton and global continental crust. Before 1.8 Ga, the majority volume (~84%) of the northeast margin of the North China Craton has formed, which is consistent with previous studies.

(4) The continental growth of the northeast margin of the North China Craton is an episodic growth, not continuously. Moreover, we give a suggestion that the mainly growth period of continental crust in the North China Craton is 2.5 Ga and 2.7 Ga, and the strongest reworking period in the North China Craton is at 1.8 Ga. After the reactivation of the North China Craton, the addition of juvenile crust was gradually increased, but the continental crust that formed at that time, was mainly the contribution of pre-existing crusts.

Acknowledgments—This study was supported by the National Natural Science Foundation of China (Grant No. 40973010) and the Special Fund for Scientific Research in the Public Interest (Grant No. 201011057-3). In addition, we will express sincere gratitude to reviewer Guochun Zhao and associate editor Oh Chang Whan.

References

Armstrong, R. L. (1991) The persistent myth of crustal growth. *Aust. J. Earth Sci.* **38**, 613–630.

Armstrong, R. L. and Harmon, R. S. (1981) Radiogenic isotopes: The case for crustal recycling on a near-steady-state no-continental-growth earth [and discussion]. *Phil. Trans. R. Soc. Lond. A* **301**, 443–472.

Bao, C., Chen, Y. L. and Li, D. P. (2012) Discorvery of the Late Permian volcanics in the Zhulazhagamaodao, northern margin of the Alxa Block. *Earth Science Frontiers* **19**, 156–163 (in Chinese with English abstract).

Bao, C., Chen, Y. L., Guo, R. and Li, D. P. (2013) U–Pb ages, Hf isotopic composition and its geological significance of detrital zircons in the floodplain sediments from Xar Moron River, Inner Mongolia. *Acta Petrol. Sinica* **29**, 3159–3172 (in Chinese with English abstract).

Belousova, E. A., Kostitsyn, Y. A., Griffin,W. L., Begg, G. C., O'Reilly, S. Y. and Pearson, N. J. (2010) The growth of the continental crust: Constraints from zircon Hf-isotope data. *Lithos* **119**, 457–466.

Blichert-Toft, J. and Albarède, F. (1997) The Lu–Hf isotope geochemistry of chondrites and the evolution of the

mantle-crust system. *Earth Planet. Sci. Lett.* **148**, 243–258.
Condie, K. C. (1998) Episodic continental growth and supercontinents: a mantle avalanche connection? *Earth Planet. Sci. Lett.* **163**, 97–108.
Condie, K. C. (2000) Episodic continental growth models: afterthoughts and extensions. *Tectonophysics* **322**, 153–162.
Condie, K. C., Bockford, M. E., Aster, R. C., Belousova, E. and Scholl, D. W. (2011) Episodic zircon ages, Hf isotopic composition, and the preservation rate of continental crust. *Geol. Soc. Am. Bull.* **123**, 951–957.
Demoux, A., Kröner, A., Liu, D. and Badarch, G. (2009) Precambrian crystalline basement in southern Mongolia as revealed by SHRIMP zircon dating. *Inter. J. Earth Sci.* **98**, 1365–1380.
Dhuime, B., Hawkesworth, C. J., Cawood, P. A. and Storey, C. D. (2012) A change in the geodynamics of continental growth 3 billion years ago. *Science* **335**, 1334–1336.
Diwu, C. R., Sun, Y. and Wang, Q. (2012) The crustal growth and evolution of North China Craton: Revealed by Hf isotopes in detrital zircons from modern rivers. *Acta Petrol. Sinica* **28**, 3520–3530.
Elhlou, S., Belousova, E., Griffin, W. L., Pearson, N. J. and O'Reilly, S. Y. (2006) Trace element and isotopic composition of GJ-red zircon standard by laser ablation. *Geochim. Cosmochim. Acta* **70** (Suppl.), 158.
Fyfe, W. S. (1978) The evolution of the Earth's crust: Modern plate tectonics to ancient hot spot tectonics? *Chem. Geol.* **23**, 89–114.
Gao, S., Rudnick, R. L., Carlson, R. W., McDonough, W. F. and Liu, Y. S. (2002) Re–Os evidence for replacement of ancient mantle lithosphere beneath the North China craton. *Earth Planet. Sci. Lett.* **198**, 307–322.
Geng, X. L., Gao, S. and Chen, B. (2011) Crustal growth of the eastern North China Craton and Sulu orogen as revealed by U–Pb dating and Hf isotopes of detrital zircons from modern rivers. *Earth Science-Journal of China University of Geosciences* **36**, 483–499 (in Chinese with English abstract).
Geng, Y. S., Du, L. and Ren, L. (2012) Growth and reworking of the early Precambrian continental crust in the North China Craton. Constraints from zircon Hf isotopes. *Gondwana Res.* **21**, 517–529.
Griffin, W. L., Pearson, N. J., Belousova, E., Jackson, S. E., Van Achterbergh, E., O'Reilly, S. Y. and Shee, S. R. (2000) The Hf isotope composition of cratonic mantle: LAM-MC-ICPMS analysis of zircon megacrysts in kimberlites. *Geochim. Cosmochim. Acta* **64**, 133–147.
Guan, H., Sun, M., Wilde, S. A., Zhou, X. and Zhai, M. (2002) SHRIMP U–Pb zircon geochronology of the Fuping Complex. implications for formation and assembly of the North China Craton. *Precambrian Res.* **113**, 1–18.
Guo, J. H., Sun, M., Chen, F. K. and Zhai, M. G. (2005) Sm–Nd and SHRIMP U–Pb zircon geochronology of high-pressure granulites in the Sanggan area, North China Craton: timing of Paleoproterozoic continental collision. *J. Asian Earth Sci.* **24**, 629–642.
Guo, J. H., Peng, P., Chen, Y., Jiao, S. J. and Windley, B. F. (2012) UHT sapphirine granulite metamorphism at 1.93–1.92 Ga caused by gabbronorite intrusions: Implications for tectonic evolution of the northern margin of the North China Craton. *Precambrian Res.* **222–223**, 124–142.
Hawkesworth, C. J. and Kemp, A. (2006) Evolution of the continental crust. *Nature* **443**, 811–817.
Hawkesworth, C. J., Dhuime, B., Pietranik, A. B., Cawood, P. A., Kemp, A. I. S. and Storey, C. D. (2010) The generation and evolution of the continental crust. *J. Geol. Soc. London* **167**, 229–248.
Hou, K. J. and Yuan, S. D. (2010) Zircon U–Pb age and Hf isotopic composition of the volcanic and sub-volcanic rocks in the Ningwu basin and their geological implications. *Acta Petrol. Sinica* **26**, 888–902 (in Chinese with English abstract).
Iizuka, T., Komiya, T., Rino, S., Maruyama, S. and Hirata, T. (2010) Detrital zircon evidence for Hf isotopic evolution of granitoid crust and continental growth. *Geochim. Cosmochim. Acta* **74**, 2450–2472.
Jackson, S. E., Pearson, N. J., Griffin, W. L. and Belousova, E. A. (2004) The application of laser ablation-inductively coupled plasma-mass spectrometry to in situ U–Pb zircon geochronology. *Chem. Geol.* **211**, 47–69.
Jian, P., Kröner, A., Windley, B. F., Zhang, Q., Zhang, W. and Zhang, L. Q. (2012) Episodic mantle melting-crustal reworking in the late Neoarchean of the northwestern North China Craton: Zircon ages of magmatic and metamorphic rocks from the Yinshan Block. *Precambrian Res.* **222–223**, 230–254.
Kemp, A., Hawkesworth, C. J., Paterson, B. A. and Kinny, P. D. (2006) Episodic growth of the Gondwana supercontinent from hafnium and oxygen isotopes in zircon. *Nature* **439**, 580–583.
Kröner, A., Wilde, S. A., Li, J. H. and Wang, K. Y. (2005) Age and evolution of a late Archean to Paleoproterozoic upper to lower crustal section in the Wutaishan/Hengshan/Fuping terrain of northern China. *J. Asian Earth Sci.* **24**, 577–595.
Kusky, T. M., Li, J. H. and Tucker, R. D. (2001) The Archean Dongwanzi ophiolite complex, North China craton. 2.505-billion-year-old oceanic crust and mantle. *Science* **292**, 1142–1145.
Kuzmichev, A., Kröner, A., Hegner, E., Dunyi, L. and Yusheng, W. (2005) The Shishkhid ophiolite, northern Mongolia: a key to the reconstruction of a Neoproterozoic island-arc system in central Asia. *Precambrian Res.* **138**, 125–150.
Li, C. D., Zhang, F. Q., Miao, L. C., Du, Y. L., Hua, Y. Q., Xu, Y. W. and Kang, S. M. (2009) Zircon SHRIMP U–Pb geochronology of the Zhangsangou formation complex in the northern margin of North China Block, and its geological significance. *Acta Geologica Sinica* **83**, 642–650 (in Chinese with English abstract).
Li, Q. L., Chen, F., Guo, J. H., Li, X. H., Yang, Y. H. and Siebel, W. (2007) Zircon ages and Nd–Hf isotopic composition of the Zhaertai Group (Inner Mongolia): evidence for early Proterozoic evolution of the northern North China Craton. *J. Asian Earth Sci.* **30**, 573–590.
Li, S. Z. and Zhao, G. C. (2007) SHRIMP U–Pb zircon geochronology of the Liaoji granitoids: Constraints on the evolution of the Paleoproterozoic Jiao-Liao-Ji belt in the Eastern Block of the North China Craton. *Precambrian Res.* **158**, 1–16.
Li, S. Z., Zhao, G. C., Sun, M., Wu, F. Y., Liu, J. Z., Hao, D. F.,

Han, Z. Z. and Luo, Y. (2004) Mesozoic, not Paleoproterozoic SHRIMP U–Pb zircon ages of two Liaoji Granites, eastern block, North China craton. *Inter. Geol. Rev.* **46**, 162–176.

Li, S. Z., Zhao, G. C., Sun, M., Han, Z. Z., Luo, Y., Hao, D. F. and Xia, X. P. (2005) Deformation history of the Paleoproterozoic Liaohe assemblage in the eastern block of the North China Craton. *J. Asian Earth Sci.* **24**, 659–674.

Li, S. Z., Zhao, G. C., Sun, M., Han, Z. Z., Zhao, G. T. and Hao, D. F. (2006) Are the South and North Liaohe Groups of North China Craton different exotic terranes? Nd isotope constraints. *Gondwana Res.* **9**, 198–208.

Li, S. Z., Zhao, G. C., Santosh, M., Liu, X., Lai, L. M., Suo, Y. H., Song, M. C. and Wang, P. C. (2012) Structural evolution of the Jiaobei Massif in the southern segment of the Jiao-Liao-Ji Belt, North China Craton. *Precambrian Res.* **200–203**, 59–73.

Liu, C. H., Zhao, G. C., Sun, M., Wu, F. Y., Yang, J. H., Yin, C. Q. and Leung, W. H. (2011a) U–Pb and Hf isotopic study of detrital zircons from the Yejishan Group of the Lüliang Complex: Constraints on the timing of collision between the Eastern and Western Blocks, North China Craton. *Sedimentary Geol.* **236**, 129–140.

Liu, C. H., Zhao, G. C., Sun, M., Zhang, J., Yin, C. Q., Wu, F. Y. and Yang, J. H. (2011b) U–Pb and Hf isotopic study of detrital zircons from the Hutuo Group of the Wutai Complex: Constraints on the timing of collision between the Eastern and Western Blocks, North China Craton. *Gondwana Res.* **20**, 106–121.

Liu, C. H., Zhao, G. C., Sun, M., Liu, F. L., Zhang, J. and Yin, C. Q. (2012a) Zircons U–Pb and Lu–Hf isotopic and whole-rock geochemical constraints on the Gantaohe Group in the Zanhuang Complex: Implications for the tectonic evolution of the Trans-North China Orogen. *Lithos* **146–147**, 80–92.

Liu, C. H., Zhao, G. C., Sun, M., Zhang, J. and Yin, C. Q. (2012b) U–Pb geochronology and Hf isotope geochemistry of detrital zircons from the Zhongtiao Complex: Constraints on the tectonic evolution of the Trans-North China Orogen. *Precambrian Res.* **222–223**, 159–172.

Liu, C. H., Zhao, G. C., Sun, M., Zhang, J., Yin, C. Q. and He, Y. H. (2012c) Detrital zircons U–Pb dating, Hf isotope and whole-rock geochemistry from the Songshan Group in the Dengfeng Complex: Constraints on the tectonic evolution of the Trans-North China Orogen. *Precambrian Res.* **192–195**, 1–15.

Liu, D. Y., Shen, Q. H., Zhang, Z. Q., Jahn, B. M. and Auvray, B. (1990) Archean crustal evolution in China: U–Pb geochronology of the Qianxi Complex. *Precambrian Res.* **48**, 223–244.

Liu, D. Y., Nutman, A. P., Compston, W., Wu, J. S. and Shen, Q. H. (1992) Remnants of ≥3800 Ma crust in the Chinese part of the Sino-Korean craton. *Geology* **20**, 339–342.

Liu, D. Y., Wan, Y. S., Wu, J. S., Wilde, S. A., Dong, C. Y. and Zhou, H. Y. (2007) Archean crustal evolution and the oldest rocks in the North China craton. *Geol. Bull. China* **26**, 1131–1138 (in Chinese with English abstract).

Liu, S. W., Zhang, J., Li, Q. G., Zhang, L. F., Wang, W. and Yang, P. T. (2012) Geochemistry and U–Pb zircon ages of metamorphic volcanic rocks of the Paleoproterozoic L_liang Complex and constraints on the evolution of the Trans-North China Orogen, North China Craton. *Precambrian Res.* **222–223**, 173–190.

Liu, Y., Hu, Z., Gao, S., Günther, D., Xu, J., Gao, C. and Chen, H. (2008) In situ analysis of major and trace elements of anhydrous minerals by LA-ICP-MS without applying an internal standard. *Chem. Geol.* **257**, 34–43.

Lu, S. N., Zhao, G. C., Wang, H. C. and Hao, G. J. (2008) Precambrian metamorphic basement and sedimentary cover of the North China Craton: Review. *Precambrian Res.* **160**, 77–93.

Luo, Y., Sun, M., Zhao, G. C., Li, S. Z., Xu, P., Ye, K. and Xia, X. P. (2004) LA-ICP-MS U–Pb zircon ages of the Liaohe Group in the Eastern Block of the North China Craton: constraints on the evolution of the Jiao-Liao-Ji Belt. *Precambrian Res.* **134**, 349–371.

Luo, Y., Sun, M., Zhao, G. C., Li, S. Z., Ayers, J. C., Xia, X. P. and Zhang, J. H. (2008) A comparison of U–Pb and Hf isotopic compositions of detrital zircons from the North and South Liaohe Groups: Constraints on the evolution of the Jiao-Liao-Ji Belt, North China Craton. *Precambrian Res.* **163**, 279–306.

Ludwig, K. R. (2003) ISOPLOT 3.0: A Geochronological Toolkit for Microsoft Excel, Berkeley Geochronology Center. California. Berkeley Geochronology Center Special Publication.

Ma, X., Guo, J., Liu, F., Qian, Q. and Fan, H. (2013) Zircon U–Pb ages, trace elements and Nd–Hf isotopic geochemistry of Guyang sanukitoids and related rocks: Implications for the Archean crustal evolution of the Yinshan Block, North China Craton. *Precambrian Res.* **230**, 61–78.

McCulloch, M. T. and Bennett, V. C. (1994) Progressive growth of the Earth's continental crust and depleted mantle: geochemical constraints. *Geochim. Cosmochim. Acta* **58**, 4717–4738.

McLennan, S. M. and Taylor, S. R. (1982) Geochemical constraints on the growth of the continental crust. *J. Geology* **90**, 347–361.

Moorbath, S. (1977) The oldest rocks and the growth of continents. *Sci. Am.* **236**, 92–104.

Peng, T. P., Fan, W. M. and Peng, P. X. (2012) Geochronology and geochemistry of late Archean adakitic plutons from the Taishan granite-greenstone Terrain: Implications for tectonic evolution of the eastern North China Craton. *Precambrian Res.* **208–211**, 53–71.

Peng, T. P., Wilde, S. A., Fan, W. M. and Peng, B. X. (2013) Neoarchean siliceous high-Mg basalt (SHMB) from the Taishan granite-greenstone terrane, Eastern North China Craton: Petrogenesis and tectonic implications. *Precambrian Res.* **228**, 233–249.

Rino, S., Komiya, T., Windley, B. F., Katayama, I., Motoki, A. and Hirata, T. (2004) Major episodic increases of continental crustal growth determined from zircon ages of river sands; implications for mantle overturns in the Early Precambrian. *Phys. Earth Planet. Inter.* **146**, 369–394.

Rudnick, R. L. and Fountain, D. M. (1995) Nature and composition of the continental crust: a lower crustal perspective. *Reviews of Geophysics-Richmond Virginia then Washing-*

ton **33**, 267–267.
Santosh, M., Liu, D., Shi, Y. and Liu, S. J. (2013) Paleoproterozoic accretionary orogenesis in the North China Craton: A SHRIMP zircon study. *Precambrian Res.* **227**, 29–54.
Scherer, E., Münker, C. and Mezger, K. (2001) Calibration of the lutetium-hafnium clock. *Science* **293**, 683–687.
Shen, Q. H., Geng, Y. S., Song, B. and Wan, Y. S. (2005) New information from the surface outcrops and deep crust of archean rocks of the North China and Yangtze Blocks, and Qinling-Dabie Orogenic Belt. *Acta Geologica Sinica* **79**, 616–627 (in Chinese with English abstract).
Shi, Y. R., Liu, D. Y., Miao, L. C., Zhang, F., Jian, P., Zhang, W., Hou, K. and Xu, J. (2010) Devonian A-type granitic magmatism on the northern margin of the North China Craton: SHRIMP U–Pb zircon dating and Hf-isotopes of the Hongshan granite at Chifeng, Inner Mongolia, China. *Gondwana Res.* **17**, 632–641.
Sláma, J., Košler, J., Condon, D. J., Crowley, J. L., Gerdes, A., Hanchar, J. M., Horstwood, M. S. A., Morris, G. A., Nasdala, L. and Norberg, N. (2008) Plešovice zircon—a new natural reference material for U–Pb and Hf isotopic microanalysis. *Chem. Geol.* **249**, 1–35.
Söderlund, U., Patchett, P. J., Vervoort, J. D. and Isachsen, C. E. (2003) The decay constant of ^{176}Lu determined from Lu–Hf and U–Pb isotope systematics of terrestrial Precambrian high-temperature mafic intrusions. *Meteoritics and Planetary Science Supplement* **38**, 5286.
Song, B., Nutman, A. P., Liu, D. and Wu, J. (1996) 3800 to 2500 Ma crustal evolution in the Anshan area of Liaoning Province, northeastern China. *Precambrian Res.* **78**, 79–94.
Su, B. X., Qin, K. Z., Sakyi, P. A., Liu, P. P., Tang, D. M., Malaviarachchi, S. P. K., Xiao, Q. H., Sun, H., Dai, Y. C. and Yan, H. (2011) Geochemistry and geochronology of acidic rocks in the Beishan region, NW China: Petrogenesis and tectonic implications. *J. Asian Earth Sci.* **41**, 31–43.
Sun, J. F., Yang, J. H., Wu, F. Y. and Wilde, S. A. (2012) Precambrian crustal evolution of the eastern North China Craton as revealed by U–Pb ages and Hf isotopes of detrital zircons from the Proterozoic Jing'eryu Formation. *Precambrian Res.* **200–203**, 184–208.
Tam, P. Y., Zhao, G. C., Liu, F. L., Zhou, X. W., Sun, M. and Li, S. Z. (2011) Timing of metamorphism in the Paleoproterozoic Jiao-Liao-Ji Belt: New SHRIMP U–Pb zircon dating of granulites, gneisses and marbles of the Jiaobei massif in the North China Craton. *Gondwana Res.* **19**, 150–162.
Tam, P. Y., Zhao, G. C., Zhou, X. W., Sun, M., Guo, J. H., Li, S. Z., Yin, C. Q., Wu, M. L. and He, Y. H. (2012a) Metamorphic *P–T* path and implications of high-pressure pelitic granulites from the Jiaobei massif in the Jiao-Liao-Ji Belt, North China Craton. *Gondwana Res.* **22**, 104–117.
Tam, P. Y., Zhao, G. C., Sun, M., Li, S. Z., Wu, M. L. and Yin, C. Q. (2012b) Petrology and metamorphic *P–T* path of high-pressure mafic granulites from the Jiaobei massif in the Jiao-Liao-Ji Belt, North China Craton. *Lithos* **155**, 94–109.
Tam, P. Y., Zhao, G. C., Sun, M., Li, S. Z., Iizuka, Y. and George, S. K. (2012c) Metamorphic *P–T* path and tectonic implications of medium-pressure pelitic granulites from the Jiaobei massif in the Jiao-Liao-Ji Belt, North China Craton. *Precambrian Res.* **220–221**, 177–191.
Vervoort, J. D. and Jonathan Patchett, P. (1996) Behavior of hafnium and neodymium isotopes in the crust: constraints from Precambrian crustally derived granites. *Geochim. Cosmochim. Acta* **60**, 3717–3733.
Wan, Y. S., Geng, Y. S., Liu, F. L., Shen, Q. H., Liu, D. Y. and Song, B. (2000) Age and composition of the khondalite series of the North China Craton and its adjacent area. Progress in *Precambrian Res.* **23**, 221–237.
Wan, Y. S., Liu, D. Y., Song, B., Wu, J. S., Yang, C., Zhang, Z. Q. and Geng, Y. S. (2005) Geochemical and Nd isotopic compositions of 3.8 Ga meta-quartz dioritic and trondhjemitic rocks from the Anshan area and their geological significance. *J. Asian Earth Sci.* **24**, 563–575.
Wan, Y. S., Song, B., Liu, D. Y., Wilde, S. A., Wu, J., Shi, Y. R., Yin, X. and Zhou, H. (2006a) SHRIMP U–Pb zircon geochronology of Palaeoproterozoic metasedimentary rocks in the North China Craton: Evidence for a major Late Palaeoproterozoic tectonothermal event. *Precambrian Res.* **149**, 249–271.
Wan, Y. S., Wilde, S. A., Liu, D. Y., Yang, C., Song, B. and Yin, X. (2006b) Further evidence for ~1.85 Ga metamorphism in the Central Zone of the North China Craton: SHRIMP U–Pb dating of zircon from metamorphic rocks in the Lushan area, Henan Province. *Gondwana Res.* **9**, 189–197.
Wan, Y. S., Liu, D. Y., Xu, Z., Dong, C., Wang, Z., Zhou, H., Yang, Z., Liu, Z. and Wu, J. (2008) Paleoproterozoic crustally derived carbonate-rich magmatic rocks from the Daqinshan area, North China Craton: Geological, petrographical, geochronological and geochemical (Hf, Nd, O and C) evidence. *Amer. J. Sci.* **308**, 351–378.
Wan, Y. S., Liu, D. Y., Dong, C., Xu, Z., Wang, Z., Wilde, S. A., Yang, Y. H., Liu, Z. and Zhou, H. (2009) The Precambrian Khondalite Belt in the Daqingshan area, North China Craton: evidence for multiple metamorphic events in the Palaeoproterozoic era. *Geol. Soc.* **323**, 73–97.
Wan, Y. S., Liu, D. Y., Wang, S., Dong, C., Yang, E., Wang, W., Zhou, H., Ning, Z., Du, L. and Yin, X. (2010) Juvenile magmatism and crustal recycling at the end of the Neoarchean in Western Shandong Province, North China Craton. Evidence from SHRIMP zircon dating. *Amer. J. Sci.* **310**, 1503–1552.
Wan, Y. S., Wang, S., Liu, D. Y., Wang, W., Kröner, A., Dong, C., Yang, E., Zhou, H., Hangqian, X. and Ma, M. (2012a) Redefinition of depositional ages of Neoarchean supracrustal rocks in western Shandong Province, China: SHRIMP U–Pb zircon dating. *Gondwana Res.* 21, 768–784.
Wan, Y. S., Dong, C. Y., Liu, D. Y., Kröner, A., Yang, C. H., Wang, W., Du, L. L., Xie, H. Q. and Ma, M. Z. (2012b) Zircon ages and geochemistry of late Neoarchean syenogranites in the North China Craton: A review. *Precambrian Res.* **222–223**, 265–289.
Wang, C. Y., Campbell, I. H., Allen, C. M., Williams, I. S. and Eggins, S. M. (2009) Rate of growth of the preserved North American continental crust: Evidence from Hf and O isotopes in Mississippi detrital zircons. *Geochim. Cosmochim. Acta* **73**, 712–728.
Wang, W., Liu, S. W., Bai, X., Yang, P. T., Li, Q. G. and Zhang,

L. F. (2011) Geochemistry and zircon U–Pb–Hf isotopic systematics of the Neoarchean Yixian-Fuxin greenstone belt, northern margin of the North China Craton: Implications for petrogenesis and tectonic setting. *Gondwana Res*. **20**, 64–81.

Wang, W., Liu, S. W., Wilde, S. A., Li, Q. G., Zhang, J., Xiang, B., Yang, P. T. and Guo, R. R. (2012) Petrogenesis and geochronology of Precambrian granitoid gneisses in Western Liaoning Province: Constraints on Neoarchean to early Paleoproterozoic crustal evolution of the North China Craton. *Precambrian Res*. **222–223**, 290–311.

Wang, W., Yang, E., Zhai, M., Wang, S., Santosh, M., Du, L., Xie, H., Lv, B. and Wan, Y. (2013) Geochemistry of ~2.7 Ga basalts from Taishan area: Constraints on the evolution of early Neoarchean granite-greenstone belt in western Shandong Province, China. *Precambrian Res*. **224**, 94–109.

Wu, F. Y., Walker, R. J., Ren, X., Sun, D. Y. and Zhou, X. (2003) Osmium isotopic constraints on the age of lithospheric mantle beneath northeastern China. *Chem. Geol*. **196**, 107–129.

Wu, F. Y., Zhao, G. C., Wilde, S. A. and Sun, D. Y. (2005) Nd isotopic constraints on crustal formation in the North China Craton. *J. Asian Earth Sci*. **24**, 523–545.

Wu, F. Y., Yang, J. H., Wilde, S. A., Liu, X. M., Guo, J. H. and Zhai, M. G. (2007) Detrital zircon U–Pb and Hf isotopic constraints on the crustal evolution of North Korea. *Precambrian Res*. **159**, 155–177.

Wu, M. L., Zhao, G. C., Sun, M., Li, S. Z., He, Y. H. and Bao, Z. A. (2013) Zircon U–Pb geochronology and Hf isotopes of major lithologies from the Yishui terrane: implications for the crustal evolution of the Eastern Block, North China Craton. *Lithos* **170–171**, 164–178.

Xia, X. P., Sun, M., Zhao, G. C., Wu, F. Y., Xu, P., Zhang, J. and Luo, Y. (2006) U–Pb and Hf isotopic study of detrital zircons from the Wulashan khondalites: constraints on the evolution of the Ordos Terrane, Western Block of the North China Craton. *Earth Planet. Sci. Lett*. **241**, 581–593.

Xie, J., Wu, F. Y. and Ding, Z. L. (2007) Detrital zircon composition of U–Pb ages and Hf isotope of the Hunshandake sandland and implications for its provenance. *Acta Petrol. Sinica* **23**, 523–528.

Yang, J., Gao, S., Gong, H. J., Zhang, H. and Xie, S. W. (2006) Detrital zircon ages of Hanjiang River: Constraints on evolution of northern Yangtze Craton, South China. *J. China Univ. Geosci*. **18**, 210–222.

Yang, J., Gao, S., Chen, C., Tang, Y., Yuan, H., Gong, H., Xie, S. and Wang, J. (2009) Episodic crustal growth of North China as revealed by U–Pb age and Hf isotopes of detrital zircons from modern rivers. *Geochim. Cosmochim. Acta* **73**, 2660–2673.

Yang, J. H., Wu, F. Y., Wilde, S. A. and Zhao, G. C. (2008) Petrogenesis and geodynamics of Late Archean magmatism in the eastern North China Craton: geochronological, geochemical and Nd–Hf isotopic evidence. *Precambrian Res*. **167**, 125–149.

Zhang, J., Zhao, G. C., Sun, M., Wilde, S. A., Li, S. Z. and Liu, S. W. (2006) High-pressure mafic granulites in the Trans-North China Orogen: Tectonic significance and age. *Gondwana Res*. **9**, 349–362.

Zhang, J., Zhao, G. C., Li, S. Z., Sun, M., Liu, S. W., Wilde, S. A., Kroner, A. and Yin, C. Q. (2007) Deformation history of the Hengshan Complex: implications for the tectonic evolution of the Trans-North China Orogen. *J. Struct. Geol*. **29**, 933–949.

Zhang, J., Zhao, G. C., Li, S. Z., Sun, M., Liu, S. W. and Yin, C. Q. (2009) Polyphase deformation of the Fuping Complex, Trans-North China Orogen: Structures, SHRIMP U–Pb zircon ages and tectonic implications. *J. Struct. Geol*. **31**, 177–193.

Zhang, J., Zhao, G. C., Li, S. Z., Sun, M. and Liu, S. W. (2012) Structural and aeromagnetic studies of the Wutai Complex: Implications for the Tectonic Evolution of the Trans-North China Orogen. *Precambrian Res*. **222–223**, 212–229.

Zhang, S. H., Zhao, Y., Song, B. and Yang, Y. H. (2007) Zircon SHRIMP U–Pb and in-situ Lu–Hf isotope analyses of a tuff from Western Beijing: evidence for missing Late Paleozoic arc volcano eruptions at the northern margin of the North China block. *Gondwana Res*. **12**, 157–165.

Zhang, Y. B., Dostal, J., Zhao, Z., Liu, C. Q. and Guo, Z. (2011) Geochronology, geochemistry and petrogenesis of mafic and ultramafic rocks from Southern Beishan area, NW China: Implications for crust-mantle interaction. *Gondwana Res*. **20**, 816–830.

Zhao, G. C. and Guo, J. H. (2012) Precambrian Geology of China: Preface. *Precambrian Res*. **222–223**, 1–12.

Zhao, G. C. and Zhai, M. G. (2013) Lithotectonic elements of Precambrian basement in the North China Craton: review and tectonic implications. *Gondwana Res*. **23**, 1207–1240.

Zhao, G. C., Wilde, S. A., Cawood, P. A. and Lu, L. Z. (1998) Thermal evolution of the Archaean basement rocks from the eastern part of the North China Craton and its bearing on tectonic setting. *Inter. Geol. Rev*. **40**, 706–721.

Zhao, G. C., Wilde, S. A., Cawood, P. A. and Lu, L. Z. (1999) Tectonothermal history of the basement rocks in the western zone of the North China Craton and its tectonic implications. *Tectonophysics* **310**, 37–53.

Zhao, G. C., Cawood, P. A., Wilde, S. A., Sun, M. and Lu, L. (2000) Metamorphism of basement rocks in the Central Zone of the North China Craton: implications for Paleoproterozoic tectonic evolution. *Precambrian Res*. **103**, 55–88.

Zhao, G. C., Wilde, S. A., Cawood, P. A. and Sun, M. (2002) SHRIMP U–Pb zircon ages of the Fuping Complex: implications for late Archean to Paleoproterozoic accretion and assembly of the North China Craton. *Amer. J. Sci*. **302**, 191–226.

Zhao, G. C., Sun, M., Wilde, S. A. and Sanzhong, L. (2005) Late Archean to Paleoproterozoic evolution of the North China Craton: key issues revisited. *Precambrian Res*. **136**, 177–202.

Zhao, G. C., Wilde, S. A., Guo, J. H., Cawood, P. A., Sun, M. and Li, X. P. (2010) Single zircon grains record two continental collisional events in the North China craton. *Precambrian Res*. **177**, 266–276.

Zhao, G. C., Sun, M., Wilde, S. A. and Li, S. Z. (2011) Assembly, accretion and breakup of the Columbia Supercontinent: records in the North China Craton revisited. *Inter. Geol. Rev*. **53**, 1331–1356.

Zheng, J., Griffin, W. L., O'Reilly, S. Y., Liou, J. G., Zhang, R. Y. and Lu, F. (2005) Late Mesozoic–Eocene mantle replacement beneath the eastern North China Craton: evidence from the Paleozoic and Cenozoic peridotite xenoliths. *Inter. Geol. Rev*. **47**, 457–472.

Zheng, Y. F., Xiao, W. J. and Zhao, G. C. (2013) Introduction to Tectonics of China. *Gondwana Res*. **23**, 1189–1206.

Zhou, J. B., Wilde, S. A., Zhao, G. C., Zheng, C. Q., Jin, W., Zhang, X. Z. and Cheng, H. (2008) SHRIMP U–Pb zircon dating of the Neoproterozoic Penglai Group and Archean gneisses from the Jiaobei Terrane, North China, and their tectonic implications. *Precambrian Res*. **160**, 323–340.